

Self-dual homogeneous gluon field and electromagnetic structure of pion.

Ja. V. Burdanov,

Laboratory of Nuclear Problems,
Joint Institute for Nuclear Research, 141980 Dubna, Russia,

G. V. Efimov,

Bogoliubov Laboratory of Theoretical Physics,
Joint Institute for Nuclear Research, 141980 Dubna, Russia,

and **S. N. Nedelko,**

Bogoliubov Laboratory of Theoretical Physics,
Joint Institute for Nuclear Research, 141980 Dubna, Russia

Abstract

The transition form factor $F_{\gamma\pi}(Q^2)$, decay width $\Gamma(\pi^0 \rightarrow \gamma\gamma)$ and charge form factor of pion are calculated within the model of induced nonlocal quark currents based on the assumption that the nonperturbative QCD vacuum can be characterized by a homogeneous (anti-)self-dual gluon field. It is shown that the interaction of the quark spin with the vacuum gluon field, being responsible for the chiral symmetry breaking and the spectrum of light mesons, can also play the decisive role in forming the form factor $F_{\gamma\pi}(Q^2)$ and decay width $\Gamma(\pi^0 \rightarrow \gamma\gamma)$. An asymptotic behavior of quark loops in the presence of the background gluon field for large Q^2 is discussed.

I. INTRODUCTION

Pion electromagnetic properties were intensively studied within different theoretical approaches, such as perturbative QCD [1], the factorization theorems and QCD sum rules [2]- [7], approaches based on the Bethe-Salpeter equation [11]- [13], the instanton liquid model [14], relativistic quark models [8,9], nonlocal quark model with confinement [10], and some others. The reason for this permanent interest is quite understandable: a variety of general features of strong interactions clearly manifest themselves in pion physics. First of all this relates to the mechanisms of chiral symmetry breaking in QCD and general behaviour of electromagnetic form factors of hadrons. The charged form factor played the particularly important role for explanation of the quark counting rules [15] and factorization hypothesis within QCD (for review see, e.g. [2]). The two-photon decay of neutral pion and the transition form factor relates to the triangle anomaly and is important for testing the models of QCD vacuum [1,6].

The present paper is devoted to description of electromagnetic properties of pions within the model of induced nonlocal quark currents developed in our previous papers [16,17]. Namely, we calculate the charge and transition form factors and two-photon decay constant of pion. The model is based on the assumption that the (anti-)self-dual homogeneous field [18–21]

$$\begin{aligned}\hat{B}_\mu(x) &= \hat{n}B_{\mu\nu}x_\nu, \quad \hat{n} = \lambda_3 \cos \xi + \lambda_8 \sin \xi, \\ \tilde{B}_{\mu\nu} &= \pm B_{\mu\nu}, \quad B_{\mu\rho}B_{\rho\mu} = -B^2\delta_{\mu\nu}\end{aligned}\tag{1}$$

can be considered as a dominating gluon configuration in the QCD vacuum. In other words, it is assumed that the effective potential for QCD has a minimum at nonzero strength of the background field [19,22].

Vacuum field (1) leads to spontaneous violation of a range of symmetries such as CP, colour and O(3). A satisfactory restoration of these symmetries at the hadronic scale assumes an existence of domain structures in the vacuum. In a given domain the vacuum field has a specific direction and is either self-dual or anti-self-dual, but this is uncorrelated with the specific realization of Eq.(1) in another domain. The idea of domains in the QCD vacuum was discussed in application to various homogeneous fields [18,23–25]. In complete theory the domain walls should be describable by some appropriate classical solitonic solutions of equations of motion. In the effective model under consideration this idea is realized as a prescription that different quark loops (namely, those separated by the meson lines) in a diagram must be averaged over different configurations of the vacuum field (1) independently of each other.

A consideration of both the quark-gluon dynamics in the external field (1) and its manifestations in meson properties indicates that this field provides for a picture of confinement and chiral symmetry breaking which is unexpected but looks quite self-consistent and agrees with meson phenomenology.

Being taken into account nonperturbatively, the vacuum field under consideration changes analytical properties of the quark and gluon propagators drastically and makes QCD to be a nonlocal quantum field theory. The propagators of color charged fields in the presence of field (1) are entire analytical functions in the complex momentum plane [10,16,18,22] which means an absence of quarks and gluons in the observable spectrum of hadrons. The propagators are modified essentially in the infrared region and show the usual behaviour at short distances. Consideration of the Wilson loop in the presence of this field shows that the Wilson criterion is satisfied [26] with an oscillator potential between heavy quarks. The potential arises effectively due to an interaction of the charges with vacuum field but not by virtue of gluon exchange.

Due to the (anti-)self-duality and homogeneity of the field (1) the operator $\gamma_\mu(\partial_\mu - iB_\mu)$ has an infinite set of zero eigenmodes whose contribution to the quark propagator leads to the relation between densities of quark and gluon condensates:

$$\sum_{f=1}^{N_F} \lim_{m_f \rightarrow 0} m_f \langle \bar{q}_f(x) q_f(x) \rangle = -N_F \frac{B^2}{2\pi^2}, \quad (2)$$

which is valid to all loop orders in QCD. Equation (2) indicates a non-Goldstone mechanism of chiral $SU_L(N_F) \times SU_R(N_F)$ symmetry breaking (for details see [22]). This way of violation of chiral symmetry is unusual but, as it will be discussed further below, is not in conflict with the observable meson properties [17].

Manifestations of this quark-gluon dynamics in the spectrum of collective mesonic excitations were studied in [16,17] within the model of induced nonlocal quark currents. Technically, the model is based on the bosonization of one-gluon exchange interaction of quark currents in the presence of the homogeneous (anti-)self-dual vacuum gluon field (1).

The vacuum field determines basic properties of meson spectrum in the way that is completely consistent with experimental data. Namely, due to the zero modes in the quark propagator the masses of light pseudoscalar and vector mesons are strongly split, scalar and axial mesons as a simple $q\bar{q}$ systems in the ground state are absent in the spectrum (there are no scalar and axial analogies of pions and ρ -mesons). Zero modes affect drastically the pion weak decay and determine the correct value of constant f_π . An entireness of quark and gluon propagators results in the Regge character of the spectrum of orbital and radial excitations of light mesons. Moreover, scalar and axial mesons with appropriate masses (e.g., a_1 meson) appear in the hyper-fine structure of orbital

excitations of vector mesons. The mass of heavy quarkonium tends to be equal to sum of the masses of quarks, the heavy-light meson mass approaches a mass of a heavy quark, and the weak decay constant for pseudoscalar heavy-light mesons has asymptotic behaviour $1/\sqrt{m_Q}$, which is consistent with the Isgur-Wise symmetry. Quantitatively, the masses and decay constants of mesons from all different regions of the spectrum are described within ten percent inaccuracy. These different phenomena are displayed with the minimal set of parameters: gauge coupling constant, strength of the vacuum field and the quark masses.

This paper proceeds a systematic analysis of possible manifestations of the vacuum field (1) in meson properties. We intend to give a kind of unified description of a wide class of static (masses, decay widths) and dynamical (form factors) characteristics of different mesons with the set of parameters, that is minimal for QCD. Using the values of parameters fitted from the meson spectrum we got the electromagnetic form factors of pions to within 15% inaccuracy. .

Our main goal is to study the role of quark zero modes, induced by an interaction of quark spin with the vacuum field, in the two-photon decay and transition form factor of π^0 . The main result is an observation that the vacuum field (1) can be responsible for both of them. Via zero modes the vacuum field affects in a crucial manner the form factor and decay constant. In particular, we show that the spin-field interaction generates the triangle anomaly in the pion decay to two photons and leads to quantitatively satisfactory description of the transition form factor and decay width.

The main effect of the vacuum field under consideration in the charge form factor is an increasing of the contribution of triangle diagram to the form factor at moderately large transfer momentum Q^2 . This effect is due to the presence of the background field both in the quark propagators and nonlocal meson-quark vertices, which causes a specific interplay of translation and color gauge invariance in the quark loops. Namely, the translation $x \rightarrow x + a$ causes a shift in the field $B_{\mu\nu}x_\nu \rightarrow B_{\mu\nu}x_\nu + B_{\mu\nu}a_\nu$, which can be compensated by an appropriate gauge transformation. Therefore, only gauge invariant quantities turn out to be translation invariant. This results in nonconservation of energy-momentum in the separate vertices of Feynman diagrams, but the conservation is still held for a whole diagram if it is gauge invariant. This peculiarity changes an asymptotic behaviour of some Feynman diagrams at large momentum transfer. This is particularly relevant to the triangle diagram for the charge form factor. Usually the asymptotic behaviour $\sim (1/Q^2)^{-2}$ of this diagram is a direct consequence of the behaviour of a meson-quark vertex and quark propagator at short distances [11]. The presence of the vacuum field changes the asymptotics cardinally, and it becomes $\sim 1/(Q^2)^{1+m_q^2/B}$, where m_q is the

quark mass and B is the strength of the vacuum field. This improves the form factor at intermediate and moderately large Q^2 . However, the absolute asymptotics of the form factor within the model under consideration comes from the so-called bubble diagrams. These diagrams can be treated as describing the hard rescattering of quarks inside a pion via virtual gluon exchange. This mechanism is in agreement with the general analysis within quark counting rules and perturbative QCD [2,15].

In the next section we review shortly the model and introduce the electromagnetic interactions into its structure. Section III is devoted to calculation of transition form factor, where we analyze the role of quark zero modes. Charged form factor of pion is calculated and the manifestations of the vacuum field in asymptotics of Feynman diagrams at large momentum transfer is discussed in sect. IV. Several Appendices contain details of calculations.

II. THE MODEL OF INDUCED NONLOCAL QUARK CURRENTS

A. Basic Approximations and Notation

The functional integral for Euclidean QCD in the presence of the vacuum field (1) can be written in the form [22]

$$\begin{aligned}
Z &= N \int_{\Sigma_B} d\sigma_B \int_{\mathcal{G}} D\mu_G(G, B) \int_{\mathcal{F}} \prod_f^{N_f} Dq_f D\bar{q}_f \\
&\exp \left\{ \int d^4x \bar{q}_f(x) [i\hat{\nabla} - m_f + g\hat{G}] q_f(x) \right\}, \\
D\mu_G(G, B) &= DG \Delta_{\text{FP}}[G, B] \delta [\nabla(B)G] \exp \left\{ \int d^4x \mathcal{L}_{\text{YM}}[G + B] \right\}, \\
\hat{G} &= \gamma_\mu G_\mu, \quad \hat{\nabla} = \gamma_\mu \nabla_\mu, \quad \nabla_\mu = \partial_\mu - iB_\mu.
\end{aligned} \tag{3}$$

The vacuum field B_μ ($gB \equiv B$) is characterized by angle ξ and two spherical angles (φ, θ) defining the directions in the color and Euclidean spaces respectively. The measure of integration $d\sigma_B$ is defined as

$$\int_{\Sigma_B} d\sigma_B = \sum_{\pm} \frac{1}{(4\pi)^2} \int_0^\pi d\theta \sin \theta \int_0^{2\pi} d\varphi \int_0^{2\pi} d\xi, \tag{4}$$

where the symbol Σ_{\pm} denotes averaging over the self- and anti-self-dual configurations.

The functional space \mathcal{G} contains the quantum gauge fields G_μ^a vanishing at the space-time infinity. The fermionic functional integral spans the Grassmann algebra \mathcal{F} of square integrable quark fields. An anti-hermitean representation for Euclidean γ -matrices is adopted.

The functional integral (3) contains the intrinsic dimensionful quantity B , which is a gauge and renormalization invariant strength of the vacuum field, which by assumption minimizes the QCD effective potential (e.g., see [19,18,20]). This field strength (or gluon condensate) provides the natural reference scale for running quark masses $\bar{m}_f(\mu)$ and gauge coupling constant $\bar{\alpha}_s(\mu)$. Therefore, the strength of the vacuum field B , the quark masses and coupling constant at the scale $\mu = \sqrt{B}$ can be considered as the physical (intrinsic) parameters of QCD in representation (3). The strength B can be related to the fundamental scale Λ_{QCD} [19,22]. Values of the parameters have to be extracted from the analysis of hadron spectrum. To be able to do this one needs to rewrite representation (3) in terms of composite hadron fields, describing collective colorless excitations in the QCD vacuum. For meson fields this program has been realized in papers [16,17], where the model of bosonization, referred below as the model of induced nonlocal quark currents, has been developed, and the masses and weak decay constants of mesons from the different regions of meson spectrum have been calculated. The values of parameters and the results for meson masses are summarized in Table I and Fig. 1.

A derivation of the model goes through the following steps. Integrating over gluon fields G one can rewrite Eq. (3) in the form

$$Z = N \int_{\Sigma_B} d\sigma_B \int_{\mathcal{F}} \prod_f^{N_f} Dq_f D\bar{q}_f \exp \left\{ \int d^4x \bar{q}_f(x) (i\hat{\nabla} - m_f) q_f(x) + \sum_{n=2}^{\infty} L_n \right\}, \quad (5)$$

$$L_n = \frac{g^n}{n!} \int d^4y_1 \dots \int d^4y_n j_{\mu_1}^{a_1}(y_1) \cdot \dots \cdot j_{\mu_n}^{a_n}(y_n) G_{\mu_1 \dots \mu_n}^{a_1 \dots a_n}(y_1, \dots, y_n | B),$$

$$j_{\mu}^a(y) = \sum_f^{N_f} \bar{q}_f(x) \gamma_{\mu} t^a q_f(x). \quad (6)$$

The functions $G_{\mu_1 \dots \mu_n}^{a_1 \dots a_n}$ are the exact n -point gluon Green's functions in the external field B_{μ}^a .

The model of induced nonlocal quark currents is based on the assumption that the four-quark interaction L_2 in Eq. (5) plays the main role in the formation of mesonic $q\bar{q}$ collective modes, but the rest of terms L_n ($n > 2$) can be omitted in the first approximation. Thus, we consider Eq. (5) with the quark-quark interaction truncated up to the term L_2

$$Z = N \int_{\Sigma_B} d\sigma_B \int_{\mathcal{F}} \prod_f^{N_f} Dq_f D\bar{q}_f \exp \left\{ \int d^4x \bar{q}_f(x) (i\hat{\nabla} - m_f) q_f(x) + L_2 \right\}$$

$$L_2 = \frac{g^2}{2} \iint d^4x d^4y j_{\mu}^a(x) G_{\mu\nu}^{ab}(x, y | B) j_{\nu}^b(y). \quad (7)$$

Gluon two-point function $G_{\mu\nu}^{ab}(x, y | B)$ is approximated by the gluon propagator in the external field (1), so that the vacuum field is taken into account exactly but the radiative corrections are neglected in the model. The subsequent steps are straightforward and consist in a standard Fiertz transformation, decomposition of L_2 into an infinite series of current-current interaction terms and bosonization of the effective four-quark interactions. For details we refer to papers [16,17].

The starting point for incorporating the electromagnetic interactions into the model under consideration is the representation [17]

$$L_2 = \sum_{aJ\ell n} \sum_{j=|\ell-s_J|^{\ell+s_J}} \frac{1}{2\Lambda^2} G_{J\ell n}^2 \int d^4x \left[\mathcal{I}^{aJ\ell n j}(x) \right]^2, \quad (8)$$

where

$$\begin{aligned} a &= 0, 1, \dots, N_f, \quad J = S, P, V, A, \quad \ell = 0, 1, \dots, \quad n = 0, 1, \dots, \\ s_P &= s_S = 0, \quad s_V = s_A = 1, \\ G_{J\ell n}^2 &= C_J g^2 \frac{(\ell+1)}{2^\ell n! (\ell+n)!}, \quad C_S = C_P = 1/9, \quad C_V = C_A = 1/18 \end{aligned} \quad (9)$$

The currents $\mathcal{I}^{aJ\ell n j}$ are nonlocal, carry a complete set of quantum numbers (isospin a , spin-parity in the ground state J , orbital ℓ and total angular j momenta, and a radial number n) and has the following form

$$\begin{aligned} \mathcal{I}_{\mu_1 \dots \mu_\ell}^{bJ\ell n \ell} &= \mathcal{J}_{\mu_1 \dots \mu_\ell}^{bJ\ell n} \quad \text{for } J = S, P, \quad \ell \geq 0 \quad (j = \ell), \\ \mathcal{I}_\alpha^{bJ0n1} &= \mathcal{J}_\alpha^{bJ0n} \quad \text{for } J = V, A, \quad \ell = 0 \quad (j = 1), \\ \mathcal{I}_{\alpha\mu_1 \dots \mu_\ell}^{bJ\ell n j} &= \begin{cases} \frac{1}{(\ell+1)^2} \mathcal{P}_{\alpha\mu_1 \dots \mu_\ell} \left[\delta_{\alpha\mu_1} \mathcal{J}_{\rho, \rho\mu_2 \dots \mu_\ell}^{bJ\ell n} \right], & j = \ell - 1, \\ \frac{1}{\ell+1} \sum_{i=1}^{\ell} \left[\mathcal{J}_{\alpha, \mu_i \dots \mu_{i-1} \mu_{i+1} \dots \mu_\ell}^{bJ\ell n} - \mathcal{J}_{\mu_i, \alpha \dots \mu_{i-1} \mu_{i+1} \dots \mu_\ell}^{bJ\ell n} \right], & j = \ell, \\ \frac{1}{\ell+1} \mathcal{P}_{\alpha\mu_1 \dots \mu_\ell} \left[\mathcal{J}_{\alpha, \mu_1 \dots \mu_\ell}^{bJ\ell n} - \frac{1}{\ell+1} \delta_{\alpha\mu_1} \mathcal{J}_{\rho, \rho\mu_2 \dots \mu_\ell}^{bJ\ell n} \right], & j = \ell + 1. \end{cases} \end{aligned} \quad (10)$$

Symbol $\mathcal{P}_{\alpha\mu_1 \dots \mu_\ell}$ denotes a cyclic permutation of the indices $(\alpha\mu_1 \dots \mu_\ell)$. The currents $\mathcal{J}^{bJ\ell n}$ in Eq. (10) read

$$\begin{aligned} \mathcal{J}_{\alpha, \mu_1 \dots \mu_\ell}^{bJ\ell n}(x) &= \bar{q}_f(x) \left[V_{\mu_1 \dots \mu_\ell}^{bJ\ell n}(x) \right]_{ff'} q_{f'}(x), \\ \left[V_{\alpha, \mu_1 \dots \mu_\ell}^{bJ\ell n}(x) \right]_{ff'} &= M_{ff'}^b \Gamma_\alpha^J \left\{ \left\{ F_{n\ell} \left(\frac{\overleftrightarrow{\nabla}_{ff'}^2(x)}{\Lambda^2} \right) T_{\mu_1 \dots \mu_\ell}^{(\ell)} \left(\frac{1}{i} \frac{\overleftrightarrow{\nabla}_{ff'}(x)}{\Lambda} \right) \right\} \right\}, \\ F_{n\ell}(4s) &= s^n \int_0^1 dt t^{\ell+n} e^{st}, \\ \overleftrightarrow{\nabla}_{ff'} &= \xi_f \overleftarrow{\nabla} - \xi_{f'} \overrightarrow{\nabla}, \quad \overrightarrow{\nabla} = \overrightarrow{\partial} - iB, \quad \overleftarrow{\nabla} = \overleftarrow{\partial} + iB, \quad \xi_f = m_f / (m_f + m_{f'}), \\ \Gamma_S &= I, \quad \Gamma_P = i\gamma_5, \quad \Gamma_V^\alpha = \gamma^\alpha, \quad \Gamma_A^\alpha = \gamma_5 \gamma^\alpha. \end{aligned} \quad (11)$$

The polynomials $T_{\mu_1 \dots \mu_\ell}^{(\ell)}(x)$ are the irreducible tensors of $O(4)$. The doubled brackets in Eq. (11) mean that the covariant derivatives commute inside these brackets. For the sake of simplicity the scale $\Lambda^2 = \sqrt{3}B$ is introduced and a particular direction $n^a = \delta^{a8}$ of the vacuum field in the color space is fixed, so that:

$$\hat{B}_{\mu\rho}\hat{B}_{\rho\nu} = -v^2\Lambda^4\delta_{\mu\nu}, \quad v = \text{diag}(1/3, 1/3, 2/3). \quad (12)$$

Further details concerning above representations can be found in papers [16,17].

Form-factors $F_{n\ell}(s)$ appeared as a result of decomposition of bilocal quark currents over the orthogonal complete set of polynomials for which gluon propagator plays the role of a weight function. They are entire analytical functions in the complex s -plane, which is a manifestation of the gluon confinement. Now an interaction between quarks is expressed in terms of the nonlocal quark currents, which are elementary currents of the system in the sense of classification over quantum numbers.

B. Electromagnetic Interactions

Interaction of quarks with electromagnetic field A_μ can be introduced into representation (7) with L_2 written in the form of Eq. (8) by means of the minimal substitution (see also [8])

$$\begin{aligned} \vec{\nabla} &\rightarrow \vec{\nabla} - ie_f A(x), \\ \overleftarrow{\nabla} &\rightarrow \overleftarrow{\nabla} + ie_f A(x) \end{aligned} \quad (13)$$

both in the free quark Lagrangian and vertices $V_{aJ\ell n j}$. Here $e_f = eQ_f$, and Q is the charge matrix.

Equation (7) takes the form ($\mathcal{N} = \{aJ\ell n j\}$)

$$\begin{aligned} Z[A] &= \int d\sigma_B \int Dq D\bar{q} \exp \left\{ \int d^4x \bar{q}_f(x) [i\gamma_\mu \vec{\nabla}_\mu - m_f + e_f \gamma_\mu A_\mu(x)] q_f(x) \right. \\ &\quad \left. + \sum_{\mathcal{N}} \frac{1}{2\Lambda^2} G_{\mathcal{N}}^2 \int d^4x |\mathcal{I}_{\mathcal{N}}(x | A) - \text{Tr} V_{\mathcal{N}}(x | 0) S(x, x | 0)|^2 \right\}, \end{aligned} \quad (14)$$

where the currents $\mathcal{I}_{\mathcal{N}}(x | A)$ include electromagnetic field A through the vertex functions

$$V^{bJ\ell n}(x | A) = M^b \Gamma^J \left\{ \left\{ F_{n\ell} \left(\frac{\overleftrightarrow{D}(x)}{\Lambda^2} \right) T^{(\ell)} \left(\frac{1}{i} \frac{\overleftrightarrow{D}(x)}{\Lambda} \right) \right\} \right\}, \quad (15)$$

$$\overleftrightarrow{D}_{ff'}^\mu = \xi_f \left[\overleftarrow{\nabla}^\mu + ie_f A^\mu(x) \right] - \xi_{f'} \left[\overrightarrow{\nabla}^\mu - ie_{f'} A^\mu(x) \right], \quad (16)$$

One can check that under the gauge transformation

$$\begin{aligned}
q_f(x) &\rightarrow q'_f(x) = e^{ie_f\alpha(x)}q_f(x), \\
\bar{q}_f(x) &\rightarrow \bar{q}'_f(x) = \bar{q}_f(x)e^{-ie_f\alpha(x)}, \\
A_\mu(x) &\rightarrow A'_\mu(x) = A_\mu(x) + \partial_\mu\alpha(x)
\end{aligned} \tag{17}$$

the currents $\mathcal{I}_\mathcal{N}$ are transformed with the electric charge $(e_f - e_{f'})$ corresponding to a meson composed of q_f and $\bar{q}_{f'}$:

$$\begin{aligned}
\mathcal{I}_\mathcal{N}(x | A) &\rightarrow \mathcal{I}'_\mathcal{N}(x | A) = e^{i(e_f - e_{f'})\alpha(x)}\mathcal{I}_\mathcal{N}(x | A), \\
\mathcal{I}_\mathcal{N}^\dagger(x | A) &\rightarrow \mathcal{I}'^\dagger_\mathcal{N}(x | A) = \mathcal{I}_\mathcal{N}^\dagger(x | A)e^{-i(e_f - e_{f'})\alpha(x)}.
\end{aligned} \tag{18}$$

The current-current interaction $\mathcal{I}_\mathcal{N}^\dagger(x)\mathcal{I}_\mathcal{N}(x)$ is invariant under $U(1)$ transformations (17).

By means of the standard bosonization procedure [16,17] applied to Eq. (14) the functional integral $Z[A]$ can be represented in terms of the composite meson fields $\Phi_\mathcal{N}$

$$\begin{aligned}
Z[A] &= N \int \prod_{\mathcal{N}} D\Phi_\mathcal{N} \exp \left\{ \frac{1}{2} \iint d^4x d^4y \Phi_\mathcal{N}(x) \left[(\square - M_\mathcal{N}^2) \delta(x - y) \right. \right. \\
&\quad \left. \left. - h_\mathcal{N}^2 \Pi_\mathcal{N}^R(x - y) \right] \Phi_\mathcal{N}(y) + I_{\text{int}}[\Phi | A] \right\},
\end{aligned} \tag{19}$$

$$\begin{aligned}
I_{\text{int}} &= - \int d^4x h_\mathcal{N} \Phi_\mathcal{N}(x) [\Gamma_\mathcal{N}(x | A) - \Gamma_\mathcal{N}(x | 0)] \\
&\quad - \frac{1}{2} \int d^4x_1 \int d^4x_2 h_\mathcal{N} h_{\mathcal{N}'} \Phi_\mathcal{N}(x_1) [\Gamma_{\mathcal{N}\mathcal{N}'}(x_1, x_2 | A) - \delta_{\mathcal{N}\mathcal{N}'} \Pi_\mathcal{N}(x_1 - x_2)] \Phi_{\mathcal{N}'}(x_2) \\
&\quad - \sum_{m=3} \frac{1}{m} \int d^4x_1 \dots \int d^4x_m \prod_{k=1}^m h_{\mathcal{N}_k} \Phi_{\mathcal{N}_k}(x_k) \Gamma_{\mathcal{N}_1 \dots \mathcal{N}_m}(x_1, \dots, x_m | A), \\
\Gamma_{\mathcal{N}_1 \dots \mathcal{N}_m} &= \int d\sigma_B \text{Tr} \{ V_{\mathcal{N}_1}(x_1 | A) S(x_1, x_2 | A) \dots V_{\mathcal{N}_m}(x_m | A) S(x_m, x_1 | A) \}.
\end{aligned} \tag{20}$$

At zero electromagnetic field the effective meson action in Eq. (19) coincides with the action derived in [17]. Meson masses $M_\mathcal{N}$ are calculated by solving the equations

$$\Lambda^2 + G_\mathcal{N}^2 \tilde{\Pi}_\mathcal{N}(-M_\mathcal{N}^2) = 0,$$

where $\tilde{\Pi}_\mathcal{N}(p^2)$ is a diagonal part of the Fourier transform of the two-point function $\Gamma_{\mathcal{N}\mathcal{N}'}$ at zero electromagnetic field.

The meson-quark coupling constants are defined by the relations:

$$h_\mathcal{N}^2 = 1/\tilde{\Pi}'_\mathcal{N}(p^2)|_{p^2=-M_\mathcal{N}^2}. \tag{21}$$

The integral over directions of the field and the sum over self- and anti-self-dual configurations has been transferred to the exponent in Eq. (19) and included into the vertices Γ , Eq. (20). This assumes that the vacuum field configurations in the different (separated by meson lines) quark loops are considered as independent from each other. Such a prescription should reflect effectively the domain structures in the vacuum.

To get various meson-photon amplitudes one has to decompose the vertex functionals $\Gamma_{\mathcal{N}_1 \dots \mathcal{N}_m}$ into a series over the electromagnetic field A , as is shown schematically in Fig. 2. This is achieved by a decomposition of the quark propagators,

$$S_f(x, y|A) = S_f(x, y) + \sum_{n=1}^{\infty} e^n \int d^4 z_1 \dots \int d^4 z_n S_f(x, z_1) \gamma_{\mu_1} A_{\mu_1}(z_1) \dots \gamma_{\mu_n} A_{\mu_n}(z_n) S_f(z_n, y), \quad (22)$$

and vertices

$$V_{\mathcal{N}}(x|A) = V_{\mathcal{N}}(x) + \sum_{n=1}^{\infty} e^n \int d^4 z_1 \dots \int d^4 z_n V_{\mathcal{N}; \mu_1 \dots \mu_n}^{(n)}(x, z_1, \dots, z_n) A_{\mu_1}(z_1) \dots A_{\mu_n}(z_n). \quad (23)$$

A regular procedure for calculation of the vertices $V_{\mathcal{N}; \mu_1 \dots \mu_n}^{(n)}$ is described in Appendix A.

The lowest vertex for charged pion, the case of particular importance for further calculations, comes from the current \mathcal{J}_{π^+} , Eqs. (11) and (15),

$$\begin{aligned} \mathcal{J}_{\pi^+}(x) &= \bar{d}(x) i \gamma_5 F_{00} \left(\frac{\overleftrightarrow{D}}{\Lambda^2}(x) \right) u(x) = \bar{d}(x) i \gamma_5 F_{00} \left(\frac{\overleftrightarrow{\nabla}}{\Lambda^2}(x) \right) u(x) \\ &+ i \gamma_5 e \int d^4 y \bar{d}(x) A_{\mu}(y) \Gamma_{\mu}(x, y) u(x) + O(e^2), \end{aligned} \quad (24)$$

where

$$\begin{aligned} \Gamma_{\mu}(x, y) &= \int \frac{d^4 q}{(2\pi)^4} e^{iq(x-y)} \int_0^1 \int_0^1 dt d\beta \frac{t}{4\Lambda^2} \left[2i \overleftrightarrow{\nabla}_{\mu}(x) - q_{\mu} \right] \\ &\times \exp \left\{ \frac{t}{4\Lambda^2} \left[\overleftrightarrow{\nabla}^2(x) + \beta(2i \overleftrightarrow{\nabla}(x) - q)q \right] \right\}. \end{aligned} \quad (25)$$

The first term in Eq. (24) is the nonlocal quark current in the absence of field A_{μ} but the second term describes an interaction of photon with a quark inside pion which is characterized by the form factor $\Gamma_{\mu}(x, y)$ [8].

The quark propagator in the homogeneous (anti-)self-dual gluon field $S_f(x, y)$ is a solution to equation

$$\begin{aligned} (i\gamma_{\mu} \nabla_{\mu} - m_f) S_f(x, y) &= -\delta(x - y), \\ S_f(x, y) &= e^{\frac{i}{2} x_{\mu} \hat{B}_{\mu\nu} y_{\nu}} H_f(x - y), \\ H_f(z) &= (i\gamma_{\mu} \nabla_{\mu} + m_f) \left(-\nabla^2 + m_f^2 - \sigma_{\alpha\beta} \hat{B}_{\alpha\beta} \right)^{-1} \delta(z). \end{aligned} \quad (26)$$

The term $\sigma_{\alpha\beta} \hat{B}_{\alpha\beta}$ in Eq. (26) is particularly important. It describes an interaction of a quark spin with the vacuum field and is responsible for the quark zero modes. Fourier transform of the translation invariant part H_f reads [17,22]

$$\begin{aligned}
\tilde{H}_f(p) = \frac{1}{2v\Lambda^2} \int_0^1 ds e^{-\frac{p^2}{2v\Lambda^2}s} \left(\frac{1-s}{1+s} \right)^{\frac{m_f^2}{4v\Lambda^2}} & [p_\alpha \gamma_\alpha \pm i s \gamma_5 \gamma_\alpha f_{\alpha\beta} p_\beta \\
& + m_f \left(P_\pm + P_\mp \frac{1+s^2}{1-s^2} - \frac{i}{2} \gamma_\alpha f_{\alpha\beta} \gamma_\beta \frac{s}{1-s^2} \right)], \quad (27) \\
f_{\mu\nu} = \frac{\lambda^8}{v\Lambda^2} B_{\mu\nu}, &
\end{aligned}$$

where $P_\pm = (I \pm \gamma_5)/2$ and the upper (lower) sign corresponds to (anti-)self-dual configuration.

Propagator (27) is an entire analytical function in the complex momentum plane, which is treated as quark confinement. The term $\sigma_{\alpha\beta} \hat{B}_{\alpha\beta}$ in Eq. (26) is particularly important. It describes an interaction of a quark spin with the vacuum field and is responsible for the quark zero modes. Contribution of zero modes to the propagator is seen in Eq. (27) as a singularity of the integrand at $s = 1$ which is integrable unless $m_f = 0$.

Below we show that the spin-field interaction is of crucial importance for the transition form factor of neutral pion. The presence of the vacuum field in the phase factor in quark propagator and in covariant derivatives in the vertices turns out to be important for the charge form factor.

III. DECAY $\pi^0 \rightarrow \gamma\gamma$ AND $\gamma^*\pi^0 \rightarrow \gamma$ TRANSITION FORM FACTOR

A vertex relevant to the interaction of neutral pion and two photons with momenta p , k_1 and k_2 , correspondingly, has the following general structure

$$T_\pi^{\mu\nu}(p, k_1, k_2) = i\delta^{(4)}(k_1 + k_2 - p) \epsilon^{\mu\nu\alpha\beta} k_1^\alpha k_2^\beta T_\pi(p^2, k_1^2, k_2^2), \quad (28)$$

where $T_\pi(p^2, k_1^2, k_2^2)$ is a scalar function. It should be remembered that we have started with the Euclidean formulation of QCD, and k_1 , k_2 and p are Euclidean momenta.

For $\gamma^*\pi^0 \rightarrow \gamma$ transition the final photon γ is on the mass shell $k_2^2 = 0$, whereas $k_1^2 = Q^2 > 0$ for the virtual photon γ^* . The transition form factor $F_{\gamma\pi}(Q^2)$ is then defined as

$$F_{\gamma\pi}(Q^2) = T_\pi(-M_\pi^2, Q^2, 0). \quad (29)$$

The two-photon decay coupling constant

$$g_{\pi\gamma\gamma} = T_\pi(-M_\pi^2, 0, 0) \quad (30)$$

and the decay width

$$\Gamma(\pi^0 \rightarrow \gamma\gamma) = \frac{\pi}{4}\alpha^2 M_\pi^3 g_{\pi\gamma\gamma}^2. \quad (31)$$

correspond to kinematics with on-shell photons and pion: $k_1^2 = k_2^2 = 0$ and $p^2 = -M_\pi^2$.

As follows from the effective action in Eq. (20), the one loop approximation of the vertex (28) is described by the triangle diagram shown in Fig. 3. Other one loop diagrams with photon lines attached to the meson-quark vertex are identically equal to zero due to the parity conservation.

As has been mentioned above, the interaction of quark spin with the homogeneous vacuum field generates an infinite number of zero modes of Dirac operator and leads to a nonzero quark condensate density, which indicates a breakdown of chiral symmetry by the vacuum gluon field [22]. A contribution of zero modes to the polarization diagrams of light mesons is responsible for mass splitting between vector and pseudoscalar mesons and smallness of pion mass [17]. The main goal of this section is to show that the zero modes generate the triangle anomaly and play the decisive role in the two-photon decay of π^0 and transition form factor $F_{\gamma\pi}$. To demonstrate this qualitatively it suffices to consider the triangle diagram (Fig. 3) in the limit of vanishing quark masses $m_d = m_u \rightarrow 0$.

The quark propagator in the external (anti-)self-dual field (1) has the following standard representation in terms of the matrix elements of the projection operators \mathcal{P}_n onto the subspaces corresponding to different eigen numbers λ_n of Dirac operator in the external field [28,22]

$$S(x, y) = \sum_{n=0}^{\infty} \frac{\mathcal{P}_n(x, y)}{m + i\lambda_n}.$$

One can separate the contribution of the zero eigenmodes and normal modes to the propagator

$$\begin{aligned} S(x, y) &= S'(x, y) + S_0(x, y), \\ S'(x, y) &= i\overrightarrow{\nabla}_x \Delta(x, y) P_\pm + \Delta(x, y) i\overleftarrow{\nabla}_y P_\mp + O(m), \\ \overrightarrow{\nabla} &= \overrightarrow{\partial} - iB, \quad \overleftarrow{\nabla} = \overleftarrow{\partial} + iB, \\ S_0(x, y) &= \mathcal{P}_0(x, y)/m. \end{aligned} \quad (32)$$

Here $\Delta(x, y)$ is the scalar massless propagator in the background field (1), and $P_\pm = (1 \pm \gamma_5)/2$. The projector onto the zero mode subspace looks as

$$\begin{aligned} \mathcal{P}_0 &= \frac{n^2 B^2}{\pi^2} f(x, y) P_\mp \Sigma_\mp, \\ \Sigma_\pm &= \frac{1}{2} (1 \pm \Sigma_j b_j), \quad \Sigma_i = \frac{1}{2} \varepsilon_{ijk} \sigma_{jk}, \quad \sigma_{jk} = [\gamma_j, \gamma_k]/2i, \\ b_j &= B_j/B, \quad B_i = -\frac{1}{2} \varepsilon_{ijk} B_{jk}, \quad i, j, k = 1, 2, 3 \end{aligned} \quad (33)$$

$$f(x, y) = \exp \left\{ -\frac{1}{2} \sqrt{n^2} B(x - y)^2 + i n x_\mu B_{\mu\nu} y_\nu \right\}, \quad (34)$$

$$\int d^4 z \mathcal{P}_0(x, z) \mathcal{P}_0(z, y) = \mathcal{P}_0(x, y).$$

The projector $\mathcal{P}_0(x, y)$ contains the projection matrices P_- (self-dual field) or P_+ (anti-self-dual field) and Σ_- ($n > 0$) or Σ_+ ($n < 0$). The matrix Σ_+ (Σ_-) can be seen as the projector onto the quark state with the spin orientated along (against) the chromomagnetic field B_j . Now consider the n -point quark loop

$$\text{Tr} \Gamma_1(S_0(x_1, x_2) + S'(x_1, x_2)) \Gamma_2(S_0(x_2, x_3) + S'(x_2, x_3)) \dots \Gamma_n(S_0(x_n, x_1) + S'(x_n, x_1)), \quad (35)$$

where Γ_k are some Dirac matrices. Chiral structure of zero mode part \mathcal{P}_0 , Eq. (33), and normal mode part S' , Eq. (32), suggests that the loops with all vector vertices are regular in the massless limit (for details see [22]), while diagrams with one pseudoscalar and $n - 1$ vector vertices are singular and behaves as $1/m_u$. The second kind is just the case of Fig. 3.

Thus the triangle diagram for the amplitude (28) is proportional to $1/m_u$ as $m_u \rightarrow 0$. However, the amplitude contains also the pion-quark coupling constant h_π defined by the pion polarization function according to Eq. (21). The polarization function is simply a two-point quark loop of the form (35) with pseudoscalar vertices. In the massless limit it diverges as $1/m_u^2$ and, hence, coupling constant $h_\pi \propto m_u$. Thus the massless limit of the form factor, that is a product of coupling constant h_π and the quark loop, is nonzero: $\lim_{m_u \rightarrow 0} F_{\gamma\pi} \neq 0$. This anomaly is determined completely by a contribution of quark zero modes to triangle diagram and coupling constant.

Let us consider this important peculiarity in more details. Using the proper time representation of the quark propagator (27) and meson-quark vertex (11), evaluating the trace of Dirac matrices, calculating the loop momentum integrals and averaging over different configurations of the vacuum field, we represent the form factor $F_{\gamma\pi}(Q^2)$ as an integral over proper times t and s_1, s_2, s_3 , corresponding to the vertex and propagators, respectively (see Fig. 3):

$$F_{\gamma\pi}(Q^2) = \frac{1}{\Lambda} \frac{h_\pi}{2\sqrt{2}\pi^2} \text{Tr}_v \int_0^1 \dots \int_0^1 dt ds_1 ds_2 ds_3 \left[\left(\frac{1-s_1}{1+s_1} \right) \left(\frac{1-s_2}{1+s_2} \right) \left(\frac{1-s_3}{1+s_3} \right) \right]^{m_u^2/4v}$$

$$\times \sum_{i=1,2,3} \frac{m_u}{1-s_i^2} \Phi_i(M_\pi^2, Q^2; s, t) \exp \left[M_\pi^2 \phi(s, t) - Q^2 \varphi(s, t) \right], \quad (36)$$

$$\phi(s, t) = (2s_1 s_3 + vt(s_1 + s_3 - s_2(1 + s_1 s_3))) / 4v\chi,$$

$$\varphi(s, t) = s_2(s_3 + vt(1 + s_1 s_3)) / 2v\chi,$$

$$\chi = 2vt(1 + s_1 s_2 + s_1 s_3 + s_2 s_3) + (s_1 + s_2 + s_3 + s_1 s_2 s_3).$$

Here and below we use the shorthand notation for dimensionless ratios: $Q^2 = Q^2/\Lambda^2$, $m_u = m_u/\Lambda$, $M_\pi = M_\pi/\Lambda$. The symbol Tr_v means summation over the elements of the diagonal matrix v written in Eq. (12). The details of calculation of $F_{\gamma\pi}(Q^2)$ and an explicit form of functions $\Phi_i(M_\pi^2, Q^2; s, t)$ can be found in Appendix B.

The singularities $(1 - s_i)^{-1}$ of the integrand in Eq. (36) at $s_i \rightarrow 1$ appear from the zero mode contribution to the quark propagator (see the second line in Eq. (27)). These singularities lead to the $1/m_u$ -dependence of the integral in Eq. (36) in the limit $m_u \ll 1$:

$$F_{\gamma\pi}(Q^2) = \frac{h_\pi}{m_u} I(Q^2). \quad (37)$$

Here I does not depend on m_u . In the massless limit pion polarization function $\tilde{\Pi}_\pi(-M_\pi^2)$ looks as [17]

$$\tilde{\Pi}_\pi(-M_\pi^2) = \frac{1}{m_u^2} \frac{16\Lambda^2}{\pi^2 M_\pi^4} \text{Tr}_v v^2 \left[\exp \left\{ \frac{M_\pi^2}{8v} \right\} - \exp \left\{ \frac{M_\pi^2}{8v(1+2v)} \right\} \right]^2, \quad (38)$$

hence the effective coupling constant h_π in Eq. (37) behaves as

$$h_\pi = 1/\sqrt{\tilde{\Pi}'_\pi(-M_\pi^2)} \sim m_u, \quad (39)$$

and $F_{\gamma\pi}(Q^2)$ does not vanish as $m_u \rightarrow 0$ but approaches a constant value. The same is valid for decay width (31).

Numerical results for the form factor and decay width are represented in Fig. 4 and Table II. The model parameters are given in Table I. It should be remembered that we simply use the values of parameters fixed from the description of the meson spectrum [17]. The solid curve in Fig. 4 corresponds to Eq. (36). The radius for $\gamma^*\pi^0 \rightarrow \gamma$ transition defined as

$$\langle r_{\gamma\pi}^2 \rangle = -6 \frac{F'_{\gamma\pi}(0)}{F_{\gamma\pi}(0)},$$

is equal to .57 fm, that have to be compared with $r_{\gamma\pi}^{\text{exp}} = .65 \pm .03$ [30].

Just to illustrate the crucial role of the quark zero modes we show the form factor calculated with zero mode contribution eliminated from the quark propagator (the long dashed line). Zero modes drastically affect also the two-photon decay constant $g_{\pi\gamma\gamma}$ and decay width $\Gamma(\pi^0 \rightarrow \gamma\gamma)$, as is seen from Table II.

Above consideration supports the picture of chiral symmetry breaking due to the fermion zero modes induced by the homogeneous (anti-)self-dual vacuum gluon field, which has been developed in our previous papers [17] and [22]. We can conclude that within the model of induced nonlocal currents the experimental data for $\gamma^*\pi^0 \rightarrow \gamma$ transition form factor and two photon decay constant can be explained by the same reason as

a smallness of pion mass, splitting of the masses of vector and pseudoscalar light mesons and weak decay constants of pions and kaons. A general physical reason is an interaction of a quark spin with the vacuum homogeneous gluon field. This spin-field interaction appears to be a dominating effect in the above discussed phenomena.

It is appropriate to mention here, that, possibly, there is another, completely independent of our considerations, manifestation of an interaction of the quark spin with a long-range gluon field in the QCD vacuum. As is reported in paper [31] the experimentally observed sign of the jet handedness correlation can be naturally understood if the jet fragmentation occurs in the background of vacuum gluon field that is (almost) homogeneous within some characteristic region. The spin-field interaction plays here the leading, qualitatively important, role.

The asymptotic behaviour of the Feynman diagrams in the limit of large momentum transfer is an additional point where the homogeneous vacuum field could be seen as a relevant effect. We will pay more attention to this in the next section, where the charge form factor of pion is considered. However, just for comparison, it is advantageous to calculate the asymptotic form of the transition form factor.

A behaviour of the triangle diagram for the transition form factor in the limit $Q^2 \gg \Lambda^2$ can be easily estimated. Equation (36) can be rewritten in the form

$$F_{\gamma\pi}(Q^2/\Lambda^2) = \frac{1}{\Lambda} \int_0^1 \dots \int_0^1 dt ds_1 ds_2 ds_3 \Phi(Q^2 s_2/\Lambda^2, M_\pi/\Lambda, m_u/\Lambda; t, s_1, s_3) \\ \times \exp \left[-\frac{Q^2}{\Lambda^2} \varphi(s, t) \right], \\ \varphi(s_1, s_2, s_3, t) = s_2(s_3 + vt(1 + s_1 s_3))/2v\chi(s_1, s_2, s_3, t),$$

which just underlines that the integrand Φ depends on Q^2 and s_2 in the combination $Q^2 s_2$, where the variable s_2 corresponds to the quark propagator situated in Fig. 3 between two electromagnetic vertices. Here we have restored the dimensional notation for the masses and momentum Q . Function χ is given in Eq. (36). For any fixed values of t, s_1, s_3 , the function φ is increasing in s_2 and gets the lowest value at the point $s_2 = 0$. This corresponds to the ultraviolet regime in the space of integration variables, that is usual for large momentum asymptotics [2]. An integral over s_2 can be evaluated by the Laplace method and, for $Q^2 \gg \Lambda^2$, we arrive at relation

$$Q^2 F_{\gamma\pi}(Q^2/\Lambda^2) = C\Lambda + O(\Lambda^2/Q^2) \approx 0.2\text{Gev} + O(\Lambda^2/Q^2), \\ C = \text{Tr}_v \int_0^1 \dots \int_0^1 dt ds_1 ds_3 \int_0^\infty ds_2 \Phi(s_2, M_\pi/\Lambda, m_u/\Lambda; t, s_1, s_3) \\ \times \exp[-s_2(s_3 + vt(1 + s_1 s_3))/2v\chi(s_1, 0, s_3, t)].$$

This result has to be compared with the Brodsky-Lepage limit [1]

$$Q^2 F_{\gamma\pi}(Q^2) \rightarrow 2F_\pi = .186\text{Gev}.$$

We see that the asymptotic regime in the form factor is realized in the usual way consistent with the analysis within factorization hypothesis and QCD sum rule approaches [6].

IV. THE PION CHARGE FORM FACTOR

According to the effective action (20), the one-loop amplitude for the processes $\pi^\pm\gamma^* \rightarrow \pi^\pm$ is described by the triangle and bubble diagrams shown in Figs. 5a and 5b correspondingly. It has the following structure

$$\Lambda^\mu(k_1, k_2, q) = \delta^{(4)}(k_1 - k_2 + q) \left[(k_1 + k_2)^\mu F_1(k_1^2, k_2^2, q^2) + q_\mu F_2(k_1^2, k_2^2, q^2) \right], \quad (40)$$

where k_1 and k_2 are the pion momenta and q is a momentum of virtual photon γ^* . As is known, within the minimal substitution scheme of introduction of electromagnetic interactions the vertex Λ^μ given by a sum of triangle and bubble diagrams satisfies the Ward-Takahashi identity [8,9].

The pion charge form factor $F_\pi(Q^2)$ is defined by the relation

$$\begin{aligned} F_\pi(Q^2) &= F_\pi^\Delta(Q^2) + F_\pi^\circ(Q^2), \\ F_\pi^\Delta &= F_1^\Delta(-M_\pi^2, -M_\pi^2, Q^2), \quad F_\pi^\circ = F_1^\circ(-M_\pi^2, -M_\pi^2, Q^2). \end{aligned}$$

The details of calculation of contributions of triangle $F_\pi^\Delta(Q^2)$ and bubble $F_\pi^\circ(Q^2)$ diagrams to the form factor are relegated to Appendix C. The result expressed in the form of the proper time integrals reads:

$$\begin{aligned} F_\pi^\Delta(Q^2) &= \frac{h_\pi^2}{4\pi^2} \text{Tr}_v \int_0^1 \dots \int_0^1 dt_1 dt_2 ds_1 ds_2 ds_3 \left[\left(\frac{1-s_1}{1+s_1} \right) \left(\frac{1-s_2}{1+s_2} \right) \left(\frac{1-s_3}{1+s_3} \right) \right]^{m_u^2/4v} \\ &\times \left[Q^2 \Phi_1(M_\pi^2, Q^2; s, t) + m_u^2 \Phi_2(M_\pi^2, Q^2; s, t) + M_\pi^2 \Phi_3(M_\pi^2, Q^2; s, t) \right. \\ &\left. + \Phi_4(M_\pi^2, Q^2; s, t) \right] \exp \left[M_\pi^2 \phi(s, t) - Q^2 \varphi(s, t) \right], \quad (41) \end{aligned}$$

$$\phi = (2s_1 s_2 + 2s_1 s_3 + v(t_1 + t_2)(s_1 + s_2 + s_3 + s_1 s_2 s_3))/4v\chi,$$

$$\chi = 2v(t_1 + t_2)(1 + s_1 s_2 + s_1 s_3 + s_2 s_3) + (1 + 4v^2 t_1 t_2)(s_1 + s_2 + s_3 + s_1 s_2 s_3),$$

$$\varphi = [s_2 s_3 + vt_1 s_2(1 + s_1 s_3) + vt_2 s_3(1 + s_1 s_2) + v^2 t_1 t_2(1 + s_1 s_2 + s_1 s_3 + s_2 s_3)]/2v\chi,$$

for triangle diagram, and

$$\begin{aligned}
F_\pi^\circ(Q^2) &= \frac{h_\pi^2}{4\pi^2} \text{Tr}_v \int_0^1 \dots \int_0^1 dt_1 dt_2 ds_1 ds_2 d\beta \left[\left(\frac{1-s_1}{1+s_1} \right) \left(\frac{1-s_2}{1+s_2} \right) \left(\frac{1-s_3}{1+s_3} \right) \right]^{m_u^2/4v} \\
&\times \left[\frac{m_u^2}{(1-s_1^2)(1-s_2^2)} \Phi_1^\circ(M_\pi^2, Q^2; \beta, s, t) + \Phi_2^\circ(M_\pi^2, Q^2; \beta, s, t) \right] \\
&\times \exp \left[M_\pi^2 \phi^\circ(s, t) - Q^2 \varphi^\circ(\beta, s, t) \right] \\
\phi^\circ &= [2s_1 s_2 + v(t_1 + t_2)(s_1 + s_2)] / 4v\chi^\circ, \\
\varphi^\circ &= \frac{vt_2\beta}{2v\chi^\circ} [s_1 + vt_1(1 + s_1 s_2) + vt_2(1 - \beta)[1 + s_1 s_2 + 2vt_1(s_1 + s_2)]], \\
\chi^\circ &= 2v(t_1 + t_2)(1 + s_1 s_2) + (1 + 4v^2 t_1 t_2)(s_1 + s_2), \tag{42}
\end{aligned}$$

for bubble diagram. We have used the shorthand dimensionless notation for momentum Q and masses. Functions Φ_i and Φ_i° are written in Appendix C.

For the parameter values given in Table 1 the charge form factor defined by Eqs. (41) and (42) is plotted in Fig. 6 by the solid line. The electromagnetic radius takes the value:

$$\langle r_\pi^2 \rangle = -6 \frac{F'_\pi(0)}{F_\pi(0)}, \quad r_\pi = .524 \text{ fm.}$$

One sees that agreement with experimental data for the form factor and radius $r_\pi^{\text{exp}} = .656 \text{ fm}$ is quite satisfactory.

An improvement of the radius and form factor at small Q^2 can come from the diagram with intermediate ρ -meson (Fig. 7). It is known [8,10] that its contribution to $F_\pi(Q^2)$ can be important in the region $Q^2 < 5\text{Gev}^2$. An estimation of the diagram with ρ -meson within the model under consideration also indicates a diminishing of the form factor, which is maximal (about 6%) in the region of $Q^2 \approx 2\text{Gev}^2$.

Numerically the contribution of the bubble diagrams is very small. It is maximal at $Q^2 \sim 2\text{Gev}^2$ and is of order 10^{-3} . Thus within the model under consideration the triangle diagram gives the main contribution to the form factor for the values of Q^2 shown in Fig. 6. One sees that the calculated form factor (the solid line) smoothly approaches the experimental fit (dashed line) at large Q^2 . This behaviour seems unexpected. As is known from the studies, based on the effective meson-quark quantum field models [8–11], the triangle diagram should decay stronger than $1/Q^2$ – the asymptotics of the experimental fit. In our case, a naive estimation based on the ultraviolet behaviour of the quark propagator (27) and vertex (11) gives $(Q^2)^{-2}$. However, the homogeneous vacuum gluon field changes the asymptotics of the triangle diagram cardinally.

To demonstrate this let us consider the function F_π^Δ in the limit $Q^2 \gg \Lambda^2$. It is convenient to rewrite Eq. (41) as

$$F_\pi^\Delta(Q^2) = \frac{h_\pi^2}{4\pi^2} \text{Tr}_v \int_0^1 \dots \int_0^1 dt_1 dt_2 ds_1 ds_2 ds_3 \left[\left(\frac{1-s_2}{1+s_2} \right) \left(\frac{1-s_3}{1+s_3} \right) \right]^{m_u^2/4v}$$

$$\begin{aligned} & \times \Phi^\Delta(Q^2, M_\pi^2, m_u^2; s_i, t_i) \exp \left\{ -\frac{Q^2}{2v} \Omega(Q^2, s, t) \right\}, \\ \Phi^\Delta = & \exp(-Q^2\psi) \left[Q^2\Phi_1(M_\pi^2, Q^2; s, t) + m_u^2\Phi_2(M_\pi^2, Q^2; s, t) \right. \\ & \left. + M_\pi^2\Phi_3(M_\pi^2, Q^2; s, t) + \Phi_4(M_\pi^2, Q^2; s, t) \right]. \end{aligned} \quad (43)$$

Function Ω has the form

$$\Omega = 2v(\varphi - \psi) + \frac{m_u^2}{2Q^2} \ln \frac{1+s_1}{1-s_1} = \frac{1-s_1}{A_1+s_1A_2} + \frac{m_u^2}{2Q^2} \ln \frac{1+s_1}{1-s_1}, \quad (44)$$

where A_1 and A_2 are functions of $t_1, t_2, s_2,$ and s_3 and do not depend on s_1 . Function ϕ is given in Eq. (41), and

$$\psi = [s_1s_2s_3 + vt_1s_2(s_1 + s_3) + vt_2s_3(s_1 + s_2) + v^2t_1t_2(s_1 + s_2 + s_3 + s_1s_2s_3)]/2v\chi$$

comes from the hyperbolic functions which have appeared in the integrand due to averaging of the quark loop over directions of the vacuum field. For details we refer to Eqs. (58) and (64) in Appendices B and C. We simply joined the exponentially increasing part of these hyperbolic functions with the exponent in Eq. (41). It should be stressed that the origin of such an exponentially increasing with $Q^2 \rightarrow \infty$ terms in the integrand is the presence of phase factor $\exp(ix_\mu B_{\mu\nu} y_\nu)$ in the quark propagator (27) and covariant derivatives $\nabla = \partial - iB$ in the vertices (11). From the physical point of view, this simply means that in the presence of external field the translation invariance holds for the gauge invariant quantities but not for the vertices and propagators separately. As is stressed in Appendix C, this is the reason why the energy-momentum is not conserved in the separate vertices, but the conservation law is still valid for a whole diagram, if it is gauge invariant.

One notices that the function Ω has a minimum at $s_1 = s_1^*$:

$$\begin{aligned} \frac{\partial \Omega}{\partial s_1} \Big|_{s_1=s_1^*} &= 0, \quad s_1^* = 1 - \frac{m_u^2}{2Q^2} (A_1 + A_2), \\ \frac{\partial^2 \Omega}{\partial s_1^2} \Big|_{s_1=s_1^*} &= \frac{2Q^2}{m_u^2 (A_1 + A_2)^2} > 0, \\ A_1 + A_2 &= \frac{(1+s_2)(1+s_3)(1+2vt_1)(1+2vt_2)}{s_2s_3 + vt_1s_2(1-s_3) + vt_2s_3(1-s_2) + v^2t_1t_2(1-s_2)(1-s_3)}, \\ \forall t_1, t_2, s_2, s_3, Q^2 \quad s_1^* &\in [0, 1], \quad \lim_{Q^2 \rightarrow \infty} s_1^* = 1, \end{aligned} \quad (45)$$

which allows to integrate over variable s_1 using the saddle-point approximation. The result is

$$\begin{aligned} F_\pi^\Delta(Q^2) &= \text{Tr}_v \int_0^1 \dots \int_0^1 dt_1 dt_2 ds_2 ds_3 \Phi^\Delta(Q^2, M_\pi^2, m_u^2; s_1^*, s_2, s_3, t_1, t_2) \\ &\times \left(\frac{m_u^2}{2Q^2} \right)^{m_u^2/4v} \frac{\sqrt{2\pi v m_u^2 (A_1 + A_2)^2}}{Q^2} \exp \left\{ -\frac{m_u^2}{4v} \left(1 - \ln \frac{A_1 + A_2}{2} \right) \right\}. \end{aligned}$$

Since functions Φ_i contained in Φ^Δ (see Eq. (41) and Appendix C) have the following asymptotic form

$$\begin{aligned}\Phi_2 \exp(-Q^2\psi) \Big|_{s_1=s_1^*} &\sim 1/Q^2(1-s_1^{*2}) = 2/m_u^2(A_1+A_2) = \text{const}, \\ \Phi_{1,3} \exp(-Q^2\psi) \Big|_{s_1=s_1^*} &\sim 1/Q^2, \quad \Phi_4 \exp(-Q^2\psi) \Big|_{s_1=s_1^*} \sim \text{const},\end{aligned}$$

hence Φ^Δ does not depend on Q^2 in the leading order

$$\lim_{Q^2 \rightarrow \infty} \Phi^\Delta(Q^2, M_\pi^2, m_u^2; s_1^*, s_2, s_3, t_1, t_2) = \Phi_{\text{as}}^\Delta(M_\pi^2, m_u^2; s_2, s_3, t_1, t_2) + O(1/Q^2).$$

Finally, the asymptotic formula for the triangle diagram reads

$$F_\pi^\Delta(Q^2/\Lambda^2) = \text{Tr}_v \frac{C^\Delta(M_\pi^2/\Lambda^2, m_u^2/\Lambda^2)}{(Q^2/\Lambda^2)^{1+m_u^2/4v\Lambda^2}}, \quad (46)$$

where factor C^Δ is independent of Q^2 ,

$$\begin{aligned}C^\Delta &= h_\pi^2 \frac{\sqrt{v}}{\sqrt{2\pi\pi}} \left(\frac{m_u}{2\Lambda}\right)^{1+m_u^2/2v\Lambda^2} e^{-m_u^2/4v\Lambda^2} \\ &\times \int_0^1 \dots \int_0^1 dt_1 dt_2 ds_2 ds_3 \Phi_{\text{as}}(M_\pi^2/\Lambda^2, m_u^2/\Lambda^2; s_2, s_3, t_1, t_2) (A_1 + A_2)^{1+m_u^2/4v\Lambda^2}.\end{aligned}$$

Here we have returned to the dimensionful notation for the masses and momentum Q . For the parameter values from Table I we obtain the following result

$$F_\pi^\Delta(Q^2/\Lambda^2) = \frac{2.96}{(Q^2/\Lambda^2)^{1.1435}}. \quad (47)$$

This asymptotic formula fits well the solid curve in Fig. 6 for $Q^2 > 5\text{Gev}^2$.

Thus the main effect of the vacuum field under consideration in the charge form factor is an increasing of the contribution of triangle diagram to the form factor at large Q^2 . As has been explained, this is clearly due to the presence of the background field both in the quark propagators and nonlocal meson-quark vertices, which causes the specific interplay of translation and color gauge invariance in the quark loops. A comparison with the large Q^2 behaviour of the $\pi\gamma\gamma$ triangle diagram, which is usual $1/Q^2$ (see the previous section), indicates that a number of nonlocal vertices in a loop is of crucial importance.

The contribution of bubble graph (see Fig. 5) to asymptotic behaviour is easy to derive if to rewrite Eq. (42) in the form

$$F_\pi^\circ(Q^2) = \text{Tr}_v \int_0^1 \dots \int_0^1 dt_1 dt_2 ds_1 ds_2 d\beta \Phi^\circ(Q^2\beta, M_\pi^2, m_u^2; s_i, t_i) \exp\{-Q^2\varphi^\circ(\beta, s_i, t_i)\},$$

which underlines that the preexponential factor Φ° depends on Q^2 in the combination $Q^2\beta$, as is seen from functions Φ_i° (see Eq. (42) and Appendix C). Here β is a proper time corresponding to the vertex operator Γ_μ given by Eq. (25). The smallest value of the function φ° corresponds to the point $\beta = 0$ for any t_1, t_2, s_1 , and s_2 :

$$\begin{aligned}\varphi^\circ(\beta, t_1, t_2, s_1, s_2) &= \beta\tilde{\varphi}^\circ(\beta, t_1, t_2, s_1, s_2), \\ \left.\frac{\partial\varphi^\circ}{\partial\beta}\right|_{\beta=0} &= \tilde{\varphi}^\circ(0, t_1, t_2, s_1, s_2) \\ &= \frac{vt_2}{2v\chi^\circ} \left[s_1 + v(t_1 + t_2)(1 + s_1s_2) + 2v^2t_1t_2(s_1 + s_2) \right] > 0.\end{aligned}$$

Therefore the leading term takes the form

$$\begin{aligned}F_\pi^\circ(Q^2/\Lambda^2) &= C^\circ(M_\pi^2/\Lambda^2, m_u^2/\Lambda^2)\frac{\Lambda^2}{Q^2} + O\left(\left(\frac{\Lambda^2}{Q^2}\right)^2\right), \\ C^\circ &= \text{Tr}_v \int_0^1 \dots \int_0^1 dt_1 dt_2 ds_1 ds_2 \int_0^\infty d\beta \Phi^\circ(\beta, M_\pi^2/\Lambda^2, m_u^2/\Lambda^2; t_1, t_2, s_1, s_2) \\ &\times \exp[-\beta\tilde{\varphi}^\circ(0, t_1, t_2, s_1, s_2)] \approx 0.3.\end{aligned}$$

We conclude that the absolute asymptotics of the charge form factor is defined by the bubble diagram. The limit $Q^2 \gg \Lambda^2$ of this diagram is due to the ultraviolet regime ($\beta \rightarrow 0$) in the vertex Γ_μ . The vertex is determined directly by the gluon propagator, and the $1/Q^2$ dependence appears as a manifestation of the ultraviolet behavior of the gluon propagator. This is in agreement with the mechanism of hard rescattering and quark counting rules [15]. Namely, the asymptotic behaviour of the form factor is determined by the one-gluon exchange between quarks inside a pion. However, in the experimentally observed region the triangle diagram dominates in the form factor.

Acknowledgments

The authors would like to thank V. Lyubovitskij and S. Mikhailov for numerous illuminating discussions. We are also grateful to A. Bakulev, A. Dorokhov, A. Efremov, M. Ivanov, N. Kochelev, P. Minkowski, R. Ruskov and S. Solunin for useful comments. J.V.B. thanks I. Anikin for discussions. This work was supported in part by the RFBR grant No. 96-02-17435-a.

V. APPENDIX A

Below we present a procedure for decomposition of the vertices $V_{aJ\ell n}$ written in Eq. (23). We will consider the vertex for pion with $\ell = n = 0$ and $\xi_f = \xi_{f'} = 1/2$. An extension to the general case is straightforward. As is seen from Eqs. (10,11) we have to decompose the operator F_{00} in a series over electromagnetic field A . The presence of the background gluon field in the vertex is irrelevant to the question under consideration. For simplicity we drop the gluon field below. At the end one have to change the partial derivatives to the covariant ones.

The most convenient way is to use the path ordered exponential representation (e_1, e_2 are the charges of u and d quarks):

$$\begin{aligned}
 F_{00} & \left[\left(\overleftrightarrow{\partial}_\mu(x) + i(e_1 + e_2)A_\mu(x) \right)^2 / 4\Lambda^2 \right] \\
 & = \int_0^1 dt P_\beta \exp \left[\frac{t}{4\Lambda^2} \int_0^1 d\beta \left(\overleftrightarrow{\partial}(x(\beta)) + i(e_1 + e_2)A(x(\beta)) \right)^2 \right] \\
 & = P_\beta \int_0^1 dt \int \frac{d^4 a}{\pi^2} e^{-\int_0^1 d\beta a^2(\beta)} e^{\frac{\sqrt{t}}{\Lambda} \int_0^1 d\beta a(\beta) \left(\overleftrightarrow{\partial} + i(e_1 + e_2)A \right)} \\
 & = P_\beta \int_0^1 dt \int d\sigma_a e^{\frac{\sqrt{t}}{\Lambda} \int_0^1 d\beta a(\beta) \left(\overleftarrow{\partial} + ie_1 A \right)} e^{-\frac{\sqrt{t}}{\Lambda} \int_0^1 d\beta a(\beta) \left(\overrightarrow{\partial} - ie_2 A \right)}
 \end{aligned}$$

Using this representation, one gets a nonambiguous decomposition for matrix element of the vertex operator:

$$\begin{aligned}
 e^{-ipx} F_{00} & \left[\left(\overleftrightarrow{\partial}_\mu(x) + i(e_1 + e_2)A_\mu(x) \right)^2 / 4\Lambda^2 \right] e^{ikx} \\
 & = \int_0^1 dt \int d\sigma_a \exp \left[-ip \left(x + \frac{\sqrt{t}}{\Lambda} \int_0^1 d\beta a(\beta) \right) + ik \left(x - \frac{\sqrt{t}}{\Lambda} \int_0^1 d\beta a(\beta) \right) \right]
 \end{aligned}$$

$$\begin{aligned}
& +i\frac{\sqrt{t}}{\Lambda}e_1\int_0^1d\beta a(\beta)A\left(x+\frac{\sqrt{t}}{\Lambda}\int_0^\beta d\beta'a(\beta')\right) \\
& +i\frac{\sqrt{t}}{\Lambda}e_2\int_0^1d\beta a(\beta)A\left(x-\frac{\sqrt{t}}{\Lambda}\int_0^\beta d\beta'a(\beta')\right)\Big] \\
& =\int_0^1dt\int d\sigma_a\exp\left\{-i(p-k)x-i\frac{\sqrt{t}}{\Lambda}(p+k)\int_0^1d\beta a(\beta)\right\} \\
& \times\left[1+i\frac{\sqrt{t}}{\Lambda}e_1\int_0^1d\beta a(\beta)A\left(x+\frac{\sqrt{t}}{\Lambda}\int_0^\beta d\beta'a(\beta')\right)\right. \\
& \left.+i\frac{\sqrt{t}}{\Lambda}e_2\int_0^1d\beta a(\beta)A\left(x-\frac{\sqrt{t}}{\Lambda}\int_0^\beta d\beta'a(\beta')\right)+O(e_1^2)+O(e_2^2)\right]. \tag{48}
\end{aligned}$$

If we now introduce Fourier transformed electromagnetic field,

$$A_\mu(y)=\int\frac{d^4q}{(2\pi)^4}e^{iqy}\tilde{A}_\mu(q),$$

then a calculation of coefficients of decomposition to any order in A is reduced to evaluation of Gaussian path integrals. These integrals can be performed expanding the paths $a_\mu(\beta)$ into trigonometric series

$$a_\mu(\beta)=a_\mu^0+\sum_{n=0}^{\infty}[u_\mu^n\cos 2\pi n\beta+v_\mu^n\sin 2\pi n\beta]=a_\mu^0+\bar{a}_\mu(\beta).$$

In the linear order in A one has to evaluate the integrals:

$$\begin{aligned}
& \int_0^1dt\int d\sigma_a\exp\left[-i(p-k)x-i\frac{\sqrt{t}}{\Lambda}a_0(p+k)\right]=\int_0^1dt\exp\left[-i(p-k)x-\frac{t}{4\Lambda^2}(p+k)^2\right] \\
& =e^{-ipx}F_{00}(-(p+k)^2)e^{ikx}=e^{-ipx}F_{00}\left(\overset{\leftrightarrow}{\partial}^2(x)\right)e^{ikx}, \\
& \int d\sigma_a a_\mu^0\exp\left[-i\frac{\sqrt{t}}{\Lambda}a_0(p+k-\beta q)\right] \\
& =-i\frac{\sqrt{t}}{2\Lambda}(p+k-\beta q)_\mu\exp\left[-\frac{t}{4\Lambda^2}(p+k-\beta q)^2\right], \\
& \int d\sigma_a\exp\left[-i\frac{\sqrt{t}}{\Lambda}a_0(p+k)+i\frac{\sqrt{t}}{\Lambda}\beta a^0q\right]=\exp\left[-\frac{t}{4\Lambda^2}(p+k-\beta q)^2\right], \\
& \int d\sigma_{\bar{a}}\exp\left[iq\frac{\sqrt{t}}{\Lambda}\int_0^\beta d\beta'\bar{a}(\beta')\right]=\exp\left[-\frac{t}{4\Lambda^2}\beta(1-\beta)q^2\right], \\
& \int d\sigma_{\bar{a}}\bar{a}_\mu\exp\left[iq\frac{\sqrt{t}}{\Lambda}\int_0^\beta d\beta'\bar{a}(\beta')\right]=i\frac{\sqrt{t}}{4\Lambda}(1-2\beta)q_\mu\exp\left[-\frac{t}{4\Lambda^2}\beta(1-\beta)q^2\right],
\end{aligned}$$

so that

$$\begin{aligned} & \int d\sigma_a a_\mu(\beta) \exp \left[-i \frac{\sqrt{t}}{\Lambda} (p+k) \int_0^1 d\beta a(\beta) + iq \frac{\sqrt{t}}{\Lambda} \int_0^\beta d\beta' a(\beta') \right] = \\ & -i \frac{\sqrt{t}}{4\Lambda} (2(p+k)_\mu - q_\mu) \exp \left[-\frac{t}{4\Lambda^2} [(p+k)^2 - \beta(2(p+k) - q)q] \right]. \end{aligned} \quad (49)$$

Inserting Eq. (49) into Eq. (48) one arrives at the representation

$$\begin{aligned} & e^{-ipx} F_{00} \left(\left[\overleftrightarrow{\partial} + i(e_1 + e_2)A \right]^2 \right) e^{ikx} = e^{-ipx} F_{00} (-(p+k)^2) e^{ikx} \\ & + (e_1 - e_2) \int \frac{d^4 q}{(2\pi)^4} e^{ix(q+k-p)} \tilde{A}_\mu(q) \int_0^1 \int_0^1 d\beta dt \frac{t}{4\Lambda^2} [2(p+k)_\mu - q_\mu] \\ & \times \exp \left[-\frac{t}{4\Lambda^2} [(p+k)^2 - \beta(2(p+k) - q)q] \right] + O(e_1^2) + O(e_2^2) = \\ & e^{-ipx} \left[F_{00} [\overleftrightarrow{\partial}^2(x)] + (e_1 - e_2) \int d^4 y A_\mu(y) \Gamma_\mu(x, y) \right] e^{ikx} + O(e_1^2) + O(e_2^2) \end{aligned}$$

with

$$\begin{aligned} \Gamma_\mu(x, y) &= \int \frac{d^4 q}{(2\pi)^4} e^{iq(x-y)} \int_0^1 \int_0^1 dt d\beta \frac{t}{4\Lambda^2} [2i \overleftrightarrow{\partial}_\mu(x) - q_\mu] \\ & \times \exp \left[\frac{t}{4\Lambda^2} \left(\overleftrightarrow{\partial}^2(x) + \beta(2i \overleftrightarrow{\partial}(x) - q)q \right) \right]. \end{aligned} \quad (50)$$

To get Eq. (25) one have to change partial derivatives to covariant derivatives ∇ with the vacuum gluon field.

Equation (50) can be written in the form

$$\begin{aligned} & e^{-ipx} \left\{ F_{00} (-(p+k)^2) + (e_1 - e_2) \int \frac{d^4 k}{(2\pi)^4} e^{iqx} \tilde{A}_\mu(q) \frac{2(p+k)_\mu - q_\mu}{2(p+k)q - q^2} \right. \\ & \left. \times \left[F_{00} (-(p+k-q)^2) - F_{00} (-(p+k)^2) \right] \right\} e^{ikx}. \end{aligned} \quad (51)$$

This formula for vertex function coincides with the representations obtained earlier in papers [8,9]. However, unlike the algorithms used in [8,9,27] above procedure can be applied regularly to calculate the higher order terms, i.e., vertices with two, three or more photons. The calculation is reduced to evaluation of Gaussian integrals.

VI. APPENDIX B

Here we give some details of calculation of the diagram in Fig 3. The contribution of the triangle diagram to the $\pi\gamma\gamma$ vertex can be represented in the form (below we use the dimensionless, i.e. divided by Λ , momenta and masses)

$$\begin{aligned}
T_\pi^{\mu\nu}(p, k_1, k_2) &= \sqrt{2}h_\pi\Lambda \int d\sigma_B \int \frac{d^4p_1 d^4p_2 d^4p_3}{(2\pi)^{12}} \tilde{R}(k_1, k_2, p; p_1, p_2, p_3) \\
&\times \text{Tr}\tau_3 i\gamma_5 \tilde{H}(p_1) \mathcal{Q}\gamma_\mu \tilde{H}(p_2) \mathcal{Q}\gamma_\nu \tilde{H}(p_3).
\end{aligned} \tag{52}$$

$$\tilde{R} = \int d^4x d^4y d^4z e^{i(px+k_1z-k_2y)} R(x, y, z; p_1, p_2, p_3), \tag{53}$$

$$\begin{aligned}
R(x, y, z; p_1, p_2, p_3) &= \exp \left[iz\hat{B}x + ip_3(z-x) \right] F_{00} \left(\frac{\overleftrightarrow{\nabla}^2(x)}{\Lambda^2} \right) \exp \left[ix\hat{B}y + ip_1(x-y) \right] \\
&\times \exp \left[iy\hat{B}z + ip_2(y-z) \right],
\end{aligned} \tag{54}$$

where $\mathcal{Q} = \text{diag}(2/3, -1/3)$ is the charge matrix, quark propagator \tilde{H} is defined by Eq. (27), and F_{00} is the vertex operator (11).

Acting by F_{00} onto the exponents in Eq. (54) and integrating over the space-time coordinates in Eq. (53), we get

$$\tilde{R} = \delta^{(4)}(p+k_1+k_2) \frac{16\pi^4}{v^4} \int_0^1 dt \exp \left[-\frac{1}{4}\beta^T \mathcal{M}_1 \beta - \frac{t}{4}(p_1+p_3)^2 \right], \tag{55}$$

where $\beta^T = (\beta_1^T \beta_2^T)$,

$$\begin{aligned}
\beta_{1\mu} &= (k_2 + p_2 - p_1)_\mu - ivt f_\mu(p_1 + p_3)/2, \\
\beta_{2\mu} &= (k_1 + p_2 - p_3)_\mu + ivt f_\mu(p_1 + p_3)/2, \\
\mathcal{M}_1 &= \frac{1}{v} \begin{pmatrix} vtI & M_1 \\ M_1^T & vtI \end{pmatrix}, \quad M_1^{\mu\nu} = vt\delta^{\mu\nu} - 2if^{\mu\nu}.
\end{aligned}$$

Inserting Eq. (55) into Eq. (52), one obtains

$$\begin{aligned}
T_\pi^{\mu\nu}(p, k_1, k_2) &= \delta^{(4)}(p+k_1+k_2) \text{Tr}_v \frac{\sqrt{2}}{v^4} h_\pi \int d\sigma_B \int_0^1 dt \int \frac{d^4p_1 d^4p_2 d^4p_3}{(2\pi)^{12}} \\
&\times \exp \left[-\frac{1}{4}\beta^T \mathcal{M}_1 \beta - \frac{t}{4}(p_1+p_3)^2 \right] \text{Tr}\tau_3 i\gamma_5 \tilde{H}(p_1) \mathcal{Q}\gamma_\mu \tilde{H}(p_2) \mathcal{Q}\gamma_\nu \tilde{H}(p_3).
\end{aligned} \tag{56}$$

A calculation of traces gives

$$\begin{aligned}
T_\pi^{\mu\nu}(p, k_1, k_2) &= i\epsilon_{\mu\nu\alpha\beta} \delta^{(4)}(k_1+k_2+p) \\
&\times \text{Tr}_v \frac{\Lambda h_\pi}{3\sqrt{2}v^7} \text{Tr}_v \int d\sigma_B \int_0^1 \dots \int_0^1 dt ds_1 ds_2 ds_3 \left[\left(\frac{1-s_1}{1+s_1} \right) \left(\frac{1-s_2}{1+s_2} \right) \left(\frac{1-s_3}{1+s_3} \right) \right]^{m_u^2/4v} \\
&\times \int \frac{d^4p_1 d^4p_2 d^4p_3}{(2\pi)^8} \mathcal{W}_{\alpha\beta}(p_1, p_2, p_3; m_u) \exp \left[-P^T \mathcal{M}_2 P + P^T Y - h(p, k_1) \right],
\end{aligned} \tag{57}$$

where

$$\begin{aligned}
\mathcal{W}^{\alpha\beta} &= \frac{m_u}{1-s_1^2} p_2^\alpha p_3^\beta - \frac{m_u}{1-s_2^2} p_1^\alpha p_3^\beta + \frac{m_u}{1-s_3^2} p_1^\alpha p_2^\beta, \\
P^T &= (p_1^T p_2^T p_3^T), \quad Y^T = (Y_1^T Y_2^T Y_3^T), \\
Y_{1\mu} &= t(p+2k_1)_\mu - if_\mu(k_1)/v, \quad Y_{2\mu} = -t(p+2k_1)_\mu + if_\mu(p)/v, \\
Y_{3\mu} &= t(p+2k_1)_\mu - if_\mu(p-k_1)/v, \quad h = tp^2/4 + tk_1^2 + tpk_1 + ik_{1\mu} f_{\mu\nu} p_\nu/v, \\
\mathcal{M}_2 &= \frac{1}{2v} \begin{pmatrix} (2vt+s_1) I & -M_2 & M_2 \\ -M_2^T & (2vt+s_2) I & -M_2 \\ M_2^T & -M_2^T & (2vt+s_3) I \end{pmatrix}, \quad M_2^{\mu\nu} = 2vt\delta^{\mu\nu} - if^{\mu\nu}.
\end{aligned}$$

Now one has to integrate over p_1, p_2, p_3 , and average over directions of the vacuum field using the following formulas

$$\begin{aligned}
\int d\sigma_B \exp(2is_2\psi p_\gamma f_{\gamma\sigma} k_{1\sigma}) &= \mathcal{F}_0(s_2\psi; k_1^2, M_\pi), \\
\int d\sigma_B \epsilon^{\mu\nu\alpha\beta} i f^{\alpha\beta} \exp(2is_2\psi p_\gamma f_{\gamma\sigma} k_{1\sigma}) &= -4\epsilon^{\mu\nu\alpha\beta} k_1^\alpha k_2^\beta \mathcal{F}_1(s_2\psi; k_1^2, M_\pi), \\
\int d\sigma_B \epsilon^{\mu\nu\alpha\beta} k_1^\alpha p^\rho i f^{\beta\rho} \exp(2is_2\psi p_\gamma f_{\gamma\sigma} k_{1\sigma}) &= 2\epsilon^{\mu\nu\alpha\beta} k_1^\alpha k_2^\beta (k_1 p) \mathcal{F}_1(s_2\psi; k_1^2, M_\pi), \\
\int d\sigma_B \epsilon^{\mu\nu\alpha\beta} p^\rho k_1^\xi f^{\alpha\rho} f^{\beta\xi} \exp(2is_2\psi p_\gamma f_{\gamma\sigma} k_{1\sigma}) &= \epsilon^{\mu\nu\alpha\beta} k_1^\alpha k_2^\beta \mathcal{F}_2(s_2\psi; k_1^2, M_\pi), \\
\mathcal{F}_0 &= \frac{1}{s_2\psi(k_1^2 + M_\pi^2)} \sinh [s_2\psi(k_1^2 + M_\pi^2)], \\
\mathcal{F}_1 &= \frac{1}{s_2\psi(k_1^2 + M_\pi^2)^2} [\cosh [s_2\psi(k_1^2 + M_\pi^2)] - \mathcal{F}_0], \\
\mathcal{F}_2 &= \mathcal{F}_0 + 4\mathcal{F}_1/s_2\psi, \\
\psi &= (s_1 s_3 + vt(s_1 + s_3))/2v\chi, \quad \chi = s_1 + s_2 + s_3 + s_1 s_2 s_3 + 2vt(1 + s_1 s_2 + s_1 s_3 + s_2 s_3).
\end{aligned}$$

These equations can be derived from the generating formula

$$\frac{1}{4\pi} \int_0^{2\pi} d\varphi \int_0^\pi d\theta \sin\theta \exp(if_{\mu\nu} J_{\mu\nu}) = \frac{\sin \sqrt{2(J_{\mu\nu} J_{\mu\nu} \pm \tilde{J}_{\mu\nu} J_{\mu\nu})}}{\sqrt{2(J_{\mu\nu} J_{\mu\nu} \pm \tilde{J}_{\mu\nu} J_{\mu\nu})}}, \quad (58)$$

where φ and θ are the spherical angles, $J_{\mu\nu}$ is an anti-symmetric tensor, $\tilde{J}_{\mu\nu}$ is a dual tensor and \pm corresponds to the self- and anti-self-dual vacuum field.

After these manipulations we arrive at the expressions for $T_\pi^{\mu\nu}(k_1, k_2, p)$, Eq. (28), and for the transition form factor $F_{\gamma\pi}(Q^2)$, Eq. (36), with functions Φ_i ($i = 1, 2, 3$) defined by the relations

$$\Phi_i(M_\pi^2, Q^2; s_1, s_2, s_3, t) = [\mathcal{F}_0 P_i + \mathcal{F}_1 R_i + \mathcal{F}_2 L_i]/6v\chi^4.$$

The polynomials P_i, R_i, L_i have the form

$$\begin{aligned}
P_1 &= vts_1^2s_2 + (s_1 + vt)[s_1 + s_2 + s_3 + 2vt(1 + s_1s_3)], \\
P_2 &= s_2[(1 + vt(s_1 + s_3))(s_2 + 2vt) + s_1(1 + 2vts_3) + s_3(1 + 2vts_1)], \\
P_3 &= vts_2s_3^2 + (s_3 + vt)[s_1 + s_2 + s_3 + 2vt(1 + s_1s_3)], \\
R_i &= M_\pi^2Q_{1i}(s, t) - Q^2Q_{2i}(s, t) + Q_{3i}(s, t), \\
Q_{11} &= (s_1 + 2vt)[2s_1s_3 + vt(s_1 + s_3 - s_2(1 + s_1s_3))], \\
Q_{12} &= 2s_1s_2s_3 - 2vt[2s_1s_3 + s_2^2(1 + s_1s_3)] - 2v^2t^2(1 + s_2^2)(s_1 + s_3), \\
Q_{13} &= (s_3 + 2vt)[2s_1s_3 + vt(s_1 + s_3 - s_2(1 + s_1s_3))], \\
Q_{21} &= s_2(s_1 + 2vt)[s_3 + vt(1 + s_1s_3)] + s_2(1 + 2vts_1)[s_1s_3 + vt(s_1 + s_3)] \\
&\quad + vt(s_1 + s_2)[s_1 + s_3 + 2vt(1 + s_1s_3)], \\
Q_{22} &= 2s_2^2s_3 + 2vts_2[s_1 - s_3 + 2s_2(1 + s_1s_3)] + 4v^2t^2s_2^2(s_1 + s_3), \\
Q_{23} &= [s_1 + s_3 + 2vt(1 + s_1s_3)][s_2s_3 + vt(s_2 - s_3)] + s_2(s_3 + 2vt)[s_3 + vt(1 + s_1s_3)] \\
&\quad - s_2(1 + 2vts_3)[s_1s_3 + vt(s_1 + s_3)], \\
Q_{31} &= 4v\chi(s_1 + 2vt), \\
Q_{32} &= 4v\chi(s_2 - 2vt), \\
Q_{33} &= 4v\chi(s_3 + 2vt), \\
L_1 &= s_2(s_1 + 2vt)[s_1s_3 + vt(s_1 + s_3)], \\
L_2 &= s_2(s_2 - 2vt)[s_1s_3 + vt(s_1 + s_3)], \\
L_3 &= s_2(s_3 + 2vt)[s_1s_3 + vt(s_1 + s_3)].
\end{aligned}$$

The polynomial χ is written in Eq. (36).

VII. APPENDIX C

As it could be seen above, the background field complicates calculation of diagrams. The reason is that in the presence of external field the translation invariance is held only for gauge invariant quantities like the diagrams in Fig. 5. This is not true for propagators or vertices separately. This means that the energy-momentum is conserved for the total diagram but not for the separate vertices and the usual Feynman rules are not valid. So that we have to begin calculation in the configuration space. The contribution of the triangle diagram to the $\pi^+\pi^-\gamma$ vertex has the form

$$\Lambda_\mu^\Delta(x, y, z) = h_\pi^2 \text{Tr} \int d\sigma_B S(z, x) i\gamma_5 F_{00} \left(\frac{\overleftrightarrow{\nabla}^2(x)}{\Lambda^2} \right) S(x, y) i\gamma_5 F_{00} \left(\frac{\overleftrightarrow{\nabla}^2(y)}{\Lambda^2} \right) S(y, z) \gamma_\mu.$$

Fourier transformed expression reads

$$\Lambda_\mu^\Delta(k_1, k_2, q) = h_\pi^2 \text{Tr}[\tau^+, \tau^-]_- \mathcal{Q} \int d\sigma_B \int \frac{d^4 p_1 d^4 p_2 d^4 p_3}{(2\pi)^{12}} \tilde{R}(k_1, k_2, q; p_1, p_2, p_3) \times i\gamma_5 \tilde{H}(p_1) i\gamma_5 \tilde{H}(p_2) \gamma_\mu \tilde{H}(p_3), \quad (59)$$

$$\tilde{R} = \int d^4 x d^4 y d^4 z e^{i(k_1 x - k_2 y + q z)} R(x, y, z; p_1, p_2, p_3),$$

$$R = \exp [iz\hat{B}x + ip_3(z-x)] F_{00} \left(\frac{\overleftrightarrow{\nabla}^2(x)}{\Lambda^2} \right) \exp [ix\hat{B}y + ip_1(x-y)] \times F_{00} \left(\frac{\overleftrightarrow{\nabla}^2(y)}{\Lambda^2} \right) \exp [iy\hat{B}z + ip_2(y-z)], \quad (60)$$

where \mathcal{Q} is the quark charge matrix, $\tilde{H}(p)$ is the quark propagator in the vacuum field (27), and F_{00} is the vertex operator (11).

The result of action of the operators F_{00} and subsequent integration over x , y and z looks as

$$\tilde{R} = \delta^{(4)}(k_1 - k_2 + q) \frac{16\pi^4}{v^4} \int_0^1 \int_0^1 \frac{dt_1 dt_2}{(1 + 4v^2 t_1 t_2)^2} \exp \left[-\frac{1}{4} \beta^T \mathcal{M}_1 \beta - g(t_1, t_2; p_1, p_2, p_3) \right], \quad (61)$$

where $\beta^T = (\beta_1^T \beta_2^T)$,

$$\mathcal{M}_1 = \frac{1}{v(1 + 4v^2 t_1 t_2)} \begin{pmatrix} v(t_1 + t_2)I & M_1 \\ M_1^T & v(t_1 + 4t_2)I \end{pmatrix},$$

$$M_1^{\mu\nu} = v(t_1 - 2t_2)\delta^{\mu\nu} - 2if^{\mu\nu},$$

$$\beta_{1\mu} = [4(k_2 + p_2 - p_1)_\mu + v^2 t_1 t_2 (k_2 + 2p_1 + 2p_2 + 2p_3)_\mu - 2ivt_1 f_\mu(p_1 + p_3) + 4ivt_2 f_\mu(p_1 + p_2)]/[4 + v^2 t_1 t_2],$$

$$\beta_{2\mu} = [4(q + p_2 - p_3)_\mu + v^2 t_1 t_2 q_\mu + 2ivt_1 f_\mu(p_1 + p_3) + 2ivt_2 f_\mu(p_1 + p_2)]/[4 + v^2 t_1 t_2],$$

$$g = [t_1(p_1 + p_3)^2 + t_2(p_1 + p_2)^2 + ivt_1 t_2 (p_1 + p_2)_\mu f_{\mu\nu}(p_1 + p_3)_\nu]/[4 + v^2 t_1 t_2].$$

Using Eq. (61) in Eq. (59) we arrive at

$$\Lambda_\mu^\Delta(k_1, k_2, q) = \delta^{(4)}(k_1 + q - k_2) \text{Tr}_v \frac{h_\pi^2}{v^4} \int_0^1 \int_0^1 \frac{dt_1 dt_2}{(1 + 4v^2 t_1 t_2)^2} \int d\sigma_B \int \frac{d^4 p_1 d^4 p_2 d^4 p_3}{(2\pi)^8} \times \text{Tr} i\gamma_5 \tilde{H}(p_1) i\gamma_5 \tilde{H}(p_2) \gamma_\mu \tilde{H}(p_3) \exp \left[-\frac{1}{4} \beta^T \mathcal{M}_1 \beta - g(t_1, t_2; p_1, p_2, p_3) \right]. \quad (62)$$

As has been discussed above, the delta function in front of the integral in Eq. (62) indicates the general conservation of energy-momentum for the total diagram. However, we have to evaluate three momentum integrals instead of one loop integral in the usual case of zero external field. These Gaussian integrals can be performed as follows.

Using representation (27) and calculating the trace of Dirac matrices, one gets

$$\begin{aligned}
\Lambda_\mu^\Delta(k_1, k_2, q) &= \text{Tr}_v \frac{h_\pi^2 \Lambda}{2v^7} \int d\sigma_B \int_0^1 \dots \int_0^1 \frac{dt_1 dt_2 ds_1 ds_2 ds_3}{(1 + 4v^2 t_1 t_2)^2} \\
&\times \left[\left(\frac{1 - s_1}{1 + s_1} \right) \left(\frac{1 - s_2}{1 + s_2} \right) \left(\frac{1 - s_3}{1 + s_3} \right) \right]^{m_u^2/4v} \\
&\times \int \frac{d^4 p_1 d^4 p_2 d^4 p_3}{(2\pi)^8} \mathcal{W}_\mu(p_1, p_2, p_3) \exp \left[-P^T \mathcal{M}_2 P + P^T Y - h(k_1, q) \right], \tag{63}
\end{aligned}$$

where $P^T = (p_1^T p_2^T p_3^T)$, $Y^T = (Y_1^T Y_2^T Y_3^T)$,

$$\begin{aligned}
Y_1^\mu &= [v(t_1 + t_2)k_1^\mu + v(2t_1 - t_2)q^\mu - i(1 - 2v^2 t_1 t_2)f^\mu(q)]/[v(1 + 4v^2 t_1 t_2)], \\
Y_2^\mu &= -[v(t_1 - t_2)k_1^\mu + v(2t_1 + t_2)q^\mu - 2iv^2 t_1 t_2 f^\mu(q) - if^\mu(k_1)]/[v(1 + 4v^2 t_1 t_2)], \\
Y_3^\mu &= [v(t_1 - t_2)k_1^\mu + v(2t_1 + t_2)q^\mu + i(1 + 2v^2 t_1 t_2)f^\mu(q) - if^\mu(k_1)]/[v(1 + 4v^2 t_1 t_2)], \\
h(k_1, q) &= [v(t_1 + t_2)k_1^2 + v(4t_1 + t_2)q^2 + 2v(2t_1 - t_2)qk_1 \\
&+ 4i(1 + v^2 t_1 t_2)q_\mu f_{\mu\nu} k_{1\nu}]/[4v(1 + 4v^2 t_1 t_2)], \\
\mathcal{M}_2 &= \frac{1}{2v(1 + 4v^2 t_1 t_2)} \begin{pmatrix} A_1 & -M_2 & M_2 \\ -M_2^T & A_2 & -N_2 \\ M_2^T & -N_2^T & A_3 \end{pmatrix}, \\
A_1^{\mu\nu} &= [2v(t_1 + t_2) + s_1(1 + 4v^2 t_1 t_2)]\delta_{\mu\nu}, \\
A_2^{\mu\nu} &= [2v(t_1 + t_2) + s_2(1 + 4v^2 t_1 t_2)]\delta_{\mu\nu}, \\
A_3^{\mu\nu} &= [2v(t_1 + t_2) + s_3(1 + 4v^2 t_1 t_2)]\delta_{\mu\nu}, \\
M_2^{\mu\nu} &= 2v(t_1 - t_2)\delta^{\mu\nu} - i(1 - 4v^2 t_1 t_2)f^{\mu\nu}, \\
N_2^{\mu\nu} &= 2v(t_1 + t_2)\delta^{\mu\nu} - i(1 + 4v^2 t_1 t_2)f^{\mu\nu},
\end{aligned}$$

and \mathcal{W}_μ has the structure:

$$\begin{aligned}
\mathcal{W}_\mu &= B_{\mu,\nu\alpha\beta} p_1^\nu p_2^\alpha p_3^\beta - \sum_{i=1}^3 C_{\mu\nu}^i p_i^\nu, \\
C_{\mu\nu}^1 &= \frac{m_u^2}{(1 - s_2^2)(1 - s_3^2)} (1 + s_1 s_2 + s_1 s_3 + s_2 s_3) [\delta_{\mu\nu}(1 - s_2 s_3) + if_{\mu\nu}(s_3 - s_2)], \\
C_{\mu\nu}^2 &= \frac{m_u^2}{(1 - s_1^2)(1 - s_3^2)} (1 + s_1 s_2 + s_1 s_3 + s_2 s_3) [\delta_{\mu\nu}(1 + s_1 s_3) + if_{\mu\nu}(s_1 + s_3)], \\
C_{\mu\nu}^3 &= \frac{m_u^2}{(1 - s_1^2)(1 - s_2^2)} (1 + s_1 s_2 + s_1 s_3 + s_2 s_3) [\delta_{\mu\nu}(1 + s_1 s_2) + if_{\mu\nu}(s_1 + s_2)], \\
B_{\mu,\nu\alpha\beta} &= (\delta_{\alpha\beta} - is_1 f_{\alpha\beta}) [\delta_{\mu\nu}(s_2 s_3 - 1) + if_{\mu\nu}(s_2 - s_3)] \\
&+ (\delta_{\nu\beta} + is_2 f_{\nu\beta}) [\delta_{\mu\alpha}(1 + s_1 s_3) + if_{\mu\alpha}(s_1 + s_3)] \\
&+ (\delta_{\alpha\nu} + is_3 f_{\alpha\nu}) [\delta_{\beta\mu}(1 + s_1 s_2) + if_{\beta\mu}(s_1 + s_2)].
\end{aligned}$$

Integrating over momenta p_1 , p_2 and p_3 , and, then, averaging over different configurations of the vacuum field by means of formulas ($k_1^2 = -M_\pi^2$, $k_2^2 = -M_\pi^2$)

$$\begin{aligned}
\int d\sigma_B \exp(2i\psi k_{1\gamma} f_{\gamma\sigma} q_\sigma) &= \mathcal{F}_0(\psi; q^2, M_\pi^2), \\
\int d\sigma_B i f_\mu(q) \exp(2i\psi k_{1\gamma} f_{\gamma\sigma} q_\sigma) &= (k_1 + k_2)_\mu q^2 \mathcal{F}_1(\psi; q^2, M_\pi^2), \\
\int d\sigma_B k_{1\alpha} q_\nu q_\beta f_{\mu\nu} f_{\alpha\beta} \exp(2i\psi k_{1\gamma} f_{\gamma\sigma} q_\sigma) &= -(k_1 + k_2)_\mu q^2 \mathcal{F}_2(\psi; q^2, M_\pi^2)/2, \\
\mathcal{F}_0 &= \frac{1}{\psi \sqrt{q^2(q^2 + 4M_\pi^2)}} \sinh \left[\psi \sqrt{q^2(q^2 + 4M_\pi^2)} \right], \\
\mathcal{F}_1 &= \frac{1}{\psi q^2(q^2 + 4M_\pi^2)} \left[\cosh \left[\psi \sqrt{q^2(q^2 + 4M_\pi^2)} \right] - \mathcal{F}_0 \right], \\
\mathcal{F}_2 &= \mathcal{F}_0 + 4\mathcal{F}_1/\psi, \\
\psi &= [s_1 s_2 s_3 + vt_1 s_2 (s_1 + s_3) + vt_2 s_3 (s_1 + s_2) + v^2 t_1 t_2 (s_1 + s_2 + s_3 + s_1 s_2 s_3)]/2v\chi, \\
\chi &= 2v(t_1 + t_2)(1 + s_1 s_2 + s_1 s_3 + s_2 s_3) + (1 + 4v^2 t_1 t_2)(s_1 + s_2 + s_3 + s_1 s_2 s_3),
\end{aligned} \tag{64}$$

we get Eq. (30) for F_π^Δ . Functions $\Phi_i(M_\pi^2, q^2; s, t)$ ($i=1,2,3$) in Eq. (30) have the form

$$\Phi_i = [\mathcal{F}_0 P_i(s, t) + \mathcal{F}_1 R_i(M_\pi^2, q^2; s, t) + \mathcal{F}_2 L_i(q^2; s, t)]/8v\chi^5.$$

$$\begin{aligned}
R_j &= q^2 \sum_{k=1,2,3} Q_{jk} \chi_k, \quad (j = 1, 3), \\
R_2 &= q^2 \left[\frac{Q_{21}}{(1 - s_1^2)(1 - s_2^2)} + \frac{Q_{22}}{(1 - s_1^2)(1 - s_3^2)} + \frac{Q_{23}}{(1 - s_2^2)(1 - s_3^2)} \right], \\
R_4 &= q^2(q^2 + 4M_\pi^2) \sum_{j=1,2,3} Q_{4j} \psi_j + q^2 Q_{44}, \\
P_j &= \sum_{k=1,2,3} Q_{jk} \psi_k, \quad (j = 1, 3) \\
P_2 &= \frac{Q_{24}}{(1 - s_1^2)(1 - s_2^2)} + \frac{Q_{25}}{(1 - s_1^2)(1 - s_3^2)} + \frac{Q_{26}}{(1 - s_2^2)(1 - s_3^2)}, \\
P_4 &= Q_{45}, \quad L_1 = L_2 = L_3 = 0, \quad L_4 = -q^2 \sum_{k=1,2,3} Q_{4k} \chi_k.
\end{aligned}$$

$$\begin{aligned}
Q_{11} &= (1 + s_1 s_2 + s_1 s_3 + s_2 s_3) [1 + 4v^2 t_1 t_2 + 2v(t_1 + t_2)s_1 + 2v^2 t_1 t_2 (1 + 4v^2 t_1 t_2)(1 - s_1^2)] \\
&+ (1 + 4v^2 t_1 t_2)(1 - s_1^2) [2vt_1 s_2 (1 + s_1 s_3) + 2vt_2 s_3 (1 + s_1 s_2) + s_2 s_3 - 1] \\
&+ v(t_1 + t_2)(1 - s_1^2) \chi, \\
Q_{12} &= -(1 + s_1 s_2 + s_1 s_3 + s_2 s_3) \\
&\times [2(1 - s_1^2)v^2 t_2^2 (1 + 4v^2 t_1^2) + (1 + 4v^2 t_1 t_2 + 2v(t_1 + t_2)s_2)(1 + 2vs_2 t_1)] \\
&+ (1 - s_2^2) [1 + s_2 s_3 + s_3(s_1 + s_2) + 4vt_1 s_2 (1 + s_1 s_3) + vt_2 (s_3(1 + s_1 s_2) - (s_1 + s_2))]
\end{aligned}$$

$$\begin{aligned}
& -4v^2t_1t_2[s_2s_3 - 1 + s_3(s_2 - s_1) + vt_2(2s_3(1 + s_1s_2) + s_2(1 + s_1s_3) + s_1 + s_3)]], \\
Q_{21} &= (1 + 4v^2t_1t_2)(1 - s_1^2)(1 - s_2^2) + v(t_1 - t_2)(s_2(1 + s_1s_2) + s_1) \\
& - (1 + v(t_1 + t_2)s_1)(s_2(s_1 + s_2) + 1), \\
Q_{24} &= -2\chi^2[-v(t_1 - t_2)s_1(s_2(1 + s_1s_2) + s_1) + v(t_1 + t_2)(s_2(s_1 + s_2) + 1) \\
& + s_1(s_2(s_1 + s_2) + 1 + s_1s_2)], \\
Q_{23} &= (1 + 4v^2t_1t_2)(1 - s_2^2)(1 - s_3^2) - v(t_1 - t_2)(s_3 - s_2)(s_2s_3 - 1) \\
& - v(t_1 + t_2)(s_3 + s_2)(s_2s_3 - 1) + 2s_2^2(1 - s_3^2) + 2s_3^2(1 - s_2^2) - (1 - s_2s_3)(1 + s_2s_3), \\
Q_{26} &= -2\chi^2[v(t_1 - t_2)(s_2 - s_3)(s_2 + s_3) + v(t_1 + t_2)(1 - s_2s_3)(1 + s_2s_3) \\
& + (s_2 + s_3)(1 - s_2s_3)], \\
Q_{31} &= 2(1 + s_1s_2 + s_1s_3 + s_2s_3)[vt_1(1 - s_1) + vt_2(1 + s_1) + s_1] \\
& [vt_1(1 + s_1) + vt_2(1 - s_1) + s_1], \\
Q_{32} &= -2(1 - s_2^2)\left[(s_1 + v(t_1 + t_2))[s_2 + s_3 + v(t_1 + t_2)(1 + s_2s_3)] \right. \\
& \left. + v^2s_1(t_1 - t_2)^2(s_2 + s_3)\right], \\
Q_{41} &= (1 + s_1s_2 + s_1s_3 + s_2s_3)[s_1(1 + 4v^2t_1t_2) + v(t_1 + t_2)(1 + s_1^2)] \\
& - (1 + 4v^2t_1t_2)(1 - s_1^2)\left[(1 - s_2s_3)(v(t_1 + t_2) + s_1) + vs_1(t_1 - t_2)(s_3 - s_2)\right], \\
Q_{42} &= (1 + s_1s_2 + s_1s_3 + s_2s_3)(s_2 + 2vt_1)[1 + 4v^2t_1t_2 + 2v(t_1 + t_2)s_2] \\
& + (1 - s_2^2)\left[s_2(s_1s_3 - 1) + 2vt_1[s_1s_2 - 1 + s_3(s_2 - s_1)] + 2vt_2s_3(s_1 + s_2) \right. \\
& \left. - 4v^2t_1t_2[s_1(s_2s_3 - 1) + s_3(s_1s_2 - 1) + vt_1(1 + s_1s_2 + s_1s_3 + s_2s_3) \right. \\
& \left. + vt_2(s_3(s_1 + s_2) - (1 + s_1s_2))\right], \\
Q_{44} &= 4v\chi[d_{41} + vt_1d_{42} + vt_2d_{43}], \\
Q_{45} &= -4v\chi[d_{44} + vt_1d_{45} + vt_2d_{46}], \\
d_{41} &= 4v(t_1 - t_2)(s_2 - s_3)(1 + s_1s_2 + s_1s_3 + s_2s_3) \\
& + (1 - 4v^2t_1t_2)\left[2(1 + s_1s_2 + s_1s_3 + s_2s_3)\left((1 + 4v^2t_1t_2)(1 + s_1s_2 + s_1s_3 + s_2s_3) \right. \right. \\
& \left. \left. - 2(1 - s_2s_3)\right) + (1 + 4v^2t_1t_2)(1 - s_1^2)(1 - s_2^2)(1 - s_3^2)\right] \\
& + (1 + 4v^2t_1t_2)(1 - s_1^2)(1 - s_2s_3)(1 + s_2s_3), \\
d_{42} &= 4(1 + s_1s_2 + s_1s_3 + s_2s_3)\left[v(t_1 - t_2)[s_1(s_2 - s_3) + s_2s_3 - 1] \right. \\
& \left. + 2(1 - 4v^2t_1t_2)s_2(1 + s_1s_3)\right] + 2vt_1(1 + 4v^2t_1t_2)s_2(1 - s_1^2)(1 - s_3^2), \\
d_{44} &= 4s_1(1 + s_1s_2 + s_1s_3 + s_2s_3)[v(t_1 - t_2)(s_3 - s_2) + (1 - 4v^2t_1t_2)(1 - s_2s_3)] \\
& + (1 + 4v^2t_1t_2)(1 - s_1^2)(s_2 + s_3)(1 - s_2s_3) \\
d_{45} &= 4(1 + s_1s_2 + s_1s_3 + s_2s_3)\left[v(t_1 - t_2)[s_1(1 - s_2s_3) + s_3 - s_2] \right.
\end{aligned}$$

$$\begin{aligned}
& +(1 - 4v^2 t_1 t_2) [s_1 (s_3 - s_2) + 1 - s_2 s_3] + (1 + 4v^2 t_1 t_2) (1 - s_1^2) (1 + s_2^2) (1 - s_3^2), \\
\chi_1 & = -4v^2 t_1 t_2 (1 - s_2^2) (1 - s_3^2) - s_2 (1 - s_3^2) (s_2 + 2vt_1) - s_3 (1 - s_2^2) (s_3 + 2vt_2), \\
\chi_2 & = -(1 + 4v^2 t_1 t_2) (1 - s_1^2) (1 - s_3^2) + 2vt_1 (s_1 + s_3) (1 + s_1 s_3) - 2vt_2 s_3 (1 - s_1^2) \\
& + s_3 (s_1 + s_3) + s_1 s_3 + 1, \\
\psi_1 & = (1 - s_2 s_3) [s_2 + s_3 + v(t_1 + t_2) (1 + s_2 s_3)] + v(t_1 - t_2) (s_2 - s_3) (s_2 + s_3), \\
\psi_2 & = [1 + s_1 s_3 + s_3 (s_1 + s_3)] (s_1 + v(t_1 + t_2)) + v(t_1 - t_2) [s_1 + s_3 + s_3 (1 + s_1 s_3)],
\end{aligned}$$

The rest of functions can be obtained by the permutations of arguments $t_1 \leftrightarrow t_2, s_2 \leftrightarrow s_3$:

$$\begin{aligned}
Q_{13}(t_1, t_2, s_1, s_2, s_3) & = Q_{12}(t_2, t_1, s_1, s_3, s_2), \quad Q_{22}(t_1, t_2, s_1, s_2, s_3) = Q_{21}(t_2, t_1, s_1, s_3, s_2), \\
Q_{25}(t_1, t_2, s_1, s_2, s_3) & = Q_{24}(t_2, t_1, s_1, s_3, s_2), \quad Q_{33}(t_1, t_2, s_1, s_2, s_3) = Q_{32}(t_2, t_1, s_1, s_3, s_2), \\
Q_{43}(t_1, t_2, s_1, s_2, s_3) & = Q_{42}(t_2, t_1, s_1, s_3, s_2), \\
d_{43}(t_1, t_2, s_1, s_2, s_3) & = d_{42}(t_2, t_1, s_1, s_3, s_2), \quad d_{46}(t_1, t_2, s_1, s_2, s_3) = d_{45}(t_2, t_1, s_1, s_3, s_2), \\
\chi_3(t_1, t_2, s_1, s_2, s_3) & = \chi_2(t_2, t_1, s_1, s_3, s_2), \quad \psi_3(t_1, t_2, s_1, s_2, s_3) = \psi_2(t_2, t_1, s_1, s_3, s_2).
\end{aligned}$$

In the configuration space the $\pi^+ \pi^- \gamma$ vertex corresponding to the bubble diagram in Fig. 5 looks as

$$\Lambda_\mu^\circ(x, y, z) = h_\pi^2 \text{Tr}([\tau^+, \tau^-]_- \mathcal{Q}) \int d\sigma_B \text{Tr}\{i\gamma_5 F_{00}(x) S(x, y) i\gamma_5 \Gamma_\mu(z, y) S(y, x)\}.$$

A calculation of this vertex is analogous to above described case of Λ_μ^Δ . Using the expression for $\Gamma_\mu(z, y)$ (25) we get Eq. (42) with

$$\Phi_i^\circ = (\mathcal{F}_0(\psi^\circ; q^2, M_\pi^2) P_i^\circ(s, t) + \mathcal{F}_1(\psi^\circ; q^2, M_\pi^2) R_i^\circ(q^2; s, t)) / (\chi^\circ)^4.$$

P_i°, R_i° are the polynomials of t, s_1, s_2 and s_3 ,

$$\begin{aligned}
R_1^\circ & = q^2 \chi^\circ (1 + s_1 s_2)^2 (s_1 s_2 + vt_1 (s_1 + s_2)) t_2 / 2, \\
R_2^\circ & = q^2 [3v(1 - 4v^2 t_1 t_2) (s_1 s_2 + vt_1 (s_1 + s_2)) - v^2 t_1 \chi^\circ] t_2 (1 + s_1 s_2), \\
P_1^\circ & = \chi^\circ (1 + s_1 s_2)^2 (s_1 - s_2) t_2 / 2 \\
P_2^\circ & = 3v(1 - 4v^2 t_1 t_2) (s_1 - s_2) t_2 (1 + s_1 s_2) / 2,
\end{aligned}$$

and

$$\begin{aligned}
\mathcal{F}_0 & = \frac{1}{\psi^\circ \sqrt{q^2 (q^2 + 4M_\pi^2)}} \sinh \left[\psi^\circ \sqrt{q^2 (q^2 + 4M_\pi^2)} \right], \\
\mathcal{F}_1 & = \frac{1}{\psi^\circ q^2 (q^2 + 4M_\pi^2)} \left\{ \cosh \left[\psi^\circ \sqrt{q^2 (q^2 + 4M_\pi^2)} \right] - \mathcal{F}_0 \right\}, \\
\psi^\circ & = vt_2 \beta (s_1 s_2 + vt_1 (s_1 + s_2)) / 2v \chi^\circ, \\
\chi^\circ & = 2v(t_1 + t_2) (1 + s_1 s_2) + (1 + 4v^2 t_1 t_2) (s_1 + s_2).
\end{aligned}$$

REFERENCES

- [1] S. Brodsky, and G. Lepage, Phys. Rev. **D24** (1981) 1808; **D22** (1980) 2157.
- [2] A. Radyushkin, Fiz. Elem. Chastits At. Yadra **20** (1989) 97.
- [3] A. Efremov, A. Radyushkin, Phys. Lett. **B94**, 245, (1980).
- [4] V. Nesterenko, A. Radyushkin, Phys. Lett. **B115**, 410, (1982); Pis'ma v ZhETPh, **39**, 576, (1984).
- [5] A. Bakulev, A. Radyushkin, Phys. Lett. **B271**, 223, (1991).
- [6] A. Radyushkin, and R. Ruskov, Sov. J. of Nucl. Phys. **56**, 103, (1993), **58**, 1440, (1995); Phys. Lett. **B374**, 173, (1996); Nucl. Phys. **B481**, 625, (1996).
- [7] B.L. Ioffe, and A.V. Smilga, Phys. Lett., **B114** (1982) 353.
- [8] H. Ito, W. Buck, and F. Gross, Phys. Lett. **B287** (1992) 23; H. Ito, W. Buck, F. Gross, Phys. Rev. **C43** (1991) 2483, Phys. Rev. **C45** (1992) 1918.
- [9] I. Anikin, V. Lyubovitskij, M. Ivanov, N. Kulimanova, Z.Phys. **C65** (1995) 681; M. Ivanov., and V. Lyubovitskij, Phys. Lett. **B408** (1997) 435.
- [10] G. Efimov and M. A. Ivanov, Int. J. Mod. Phys. **A4**, 2031 (1989): *The Quark Confinement Model of Hadrons*, IOP Publishing, Bristol and Philadelphia (1993).
- [11] C. Roberts, Nucl. Phys. **A605**, (1996) 475.
- [12] D. Kekez, and D. Klabucar, Phys. Lett. **B387** (1996) 14.
- [13] L. Kisslinger, S. Wang, Nucl. Phys. **B399**, 63, (1993).
- [14] A.E. Dorokhov, Nuovo Cim. **109A** (1996) 391.
- [15] V. Matveev, R.M. Muradyan, and A.N. Tavkhelidze, Lett. al Nuovo Cimento, **7**, (1973) 719; S.J. Brodsky, and G.R. Farrar, Phys. Rev. Lett., **31** (1973) 1153.
- [16] G.V. Efimov, and S.N. Nedelko, Phys. Rev. **D51**, 174 (1995).
- [17] Ja. Burdanov, G. Efimov, S. Nedelko, and S. Solunin, Phys. Rev. **D54**, 4483 (1996).
- [18] H. Leutwyler, Phys. Lett. **96B**, 154 (1980); Nucl. Phys. **B179**, 129 (1981).
- [19] P. Minkowski, Nucl. Phys. **B177** (1981) 203.
- [20] E. Elizalde, Nucl. Phys. **B243**, 398 (1984); E. Elizalde and J. Soto, *ibid* **B260**, 136 (1985).
- [21] J. Finjord, Nucl. Phys. **B194** (1982) 77.
- [22] G. Efimov, and S. Nedelko, Eur. Phys. J **C1**, 343 (1998).
- [23] J. Ambjorn, and P. Olesen, Nucl. Phys. **B170** (1980) 60.
- [24] P.A. Amundsen, M. Schaden, Phys.Lett. **B252** (1990) 265.
- [25] A. Chakrabarti, and F. Koukiou, Phys. Rev. **D26** (1982) 1425; A. Chakrabarti, Nucl. Phys. **B248** (1984) 209.
- [26] G.V. Efimov, A.C. Kalloniatis, and S.N. Nedelko, hep-th/9806165 (1998).
- [27] J Terning, Phys. Rev. **D44** (1991) 887.

- [28] L.S. Brown, R.D. Carlitz, D.B. Creamer, C. Lee: Phys. Rev. **D17** (1978) 1583.
- [29] J. Gronberg *et al.*, Phys. Rev. **D57** (1998) 33.
- [30] C. Bebek *et al.*, Phys. Rev. **D47**, 1693 (1978).
- [31] A. Efremov, and D. Kharzeev, Phys. Lett. **B366** (1996) 311.

TABLES

TABLE I. Parameters of the model ($\Lambda^4 = 3B^2$).

m_u (MeV)	m_d (MeV)	m_s (MeV)	m_c (MeV)	m_b (MeV)	Λ (MeV)	g
198.3	198.3	413	1650	4840	319.5	9.96

TABLE II. The two-photon decay constant $g_{\pi\gamma\gamma}$ (Gev^{-1}) and decay width $\Gamma(\pi^0 \rightarrow \gamma\gamma)$ (ev); $g_{\pi\gamma\gamma}^*, \Gamma^*$ are the values calculated without taking into account the spin-field interaction

$g_{\pi\gamma\gamma}$	$g_{\pi\gamma\gamma}^*$	$g_{\pi\gamma\gamma}^{\text{exp}} [30]$	Γ	Γ^*	$\Gamma^{\text{exp}} [30]$
0.235	0.108	0.276	6.3	1.34	8.74

FIGURES

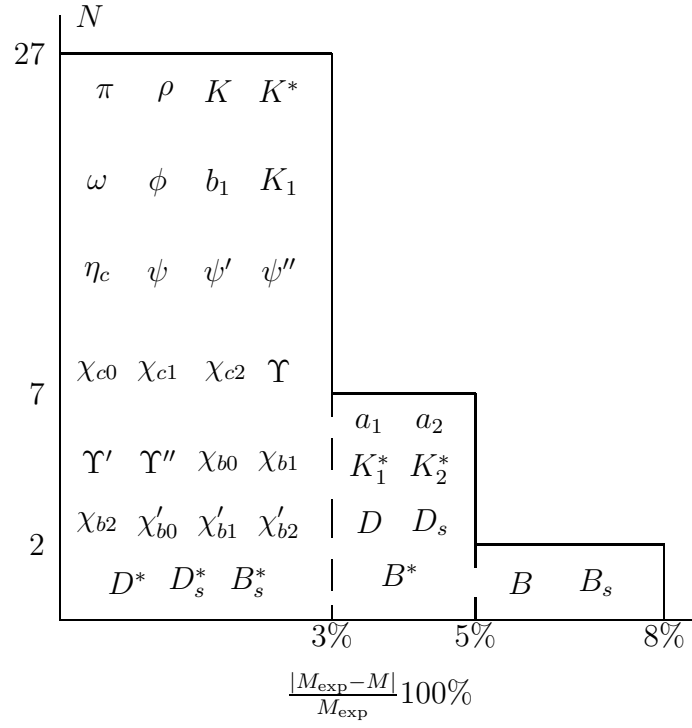


FIG. 1. A diagram illustrating accuracy of description of meson spectrum. All the masses were calculated with the values of parameters given in Table I. Parameters were fitted using the masses of π , ρ , K , K^* , ψ and Υ mesons.

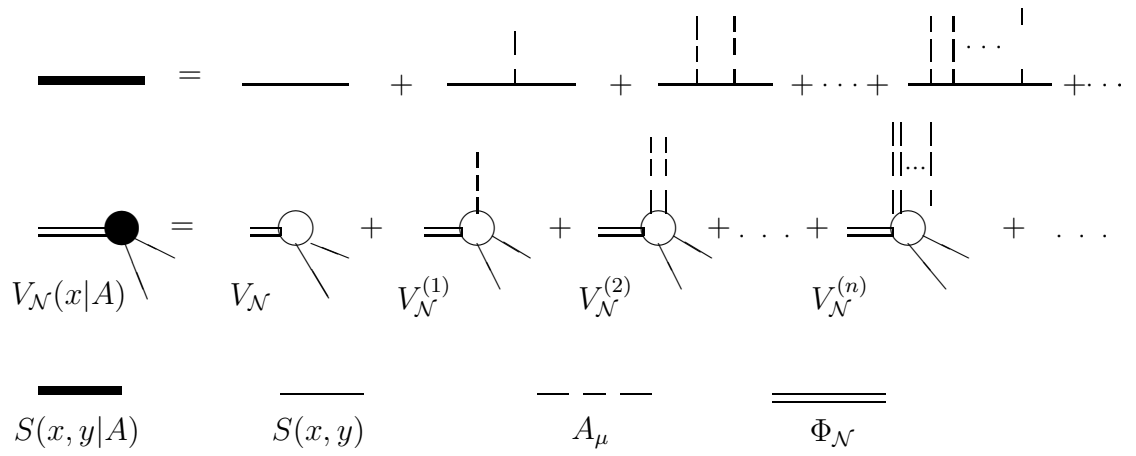


FIG. 2. A decomposition of propagators and vertices, Eqs. (22,23) into a series in electromagnetic field A . A procedure for calculation of the vertices $V_{\mathcal{N}}^{(n)}$ is described in Appendix A.

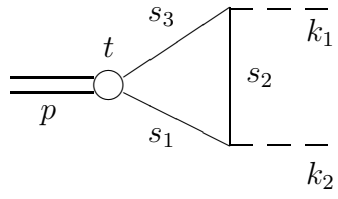


FIG. 3. The triangle diagram for the $\gamma^*\pi^0 \rightarrow \gamma$ transition form factor.

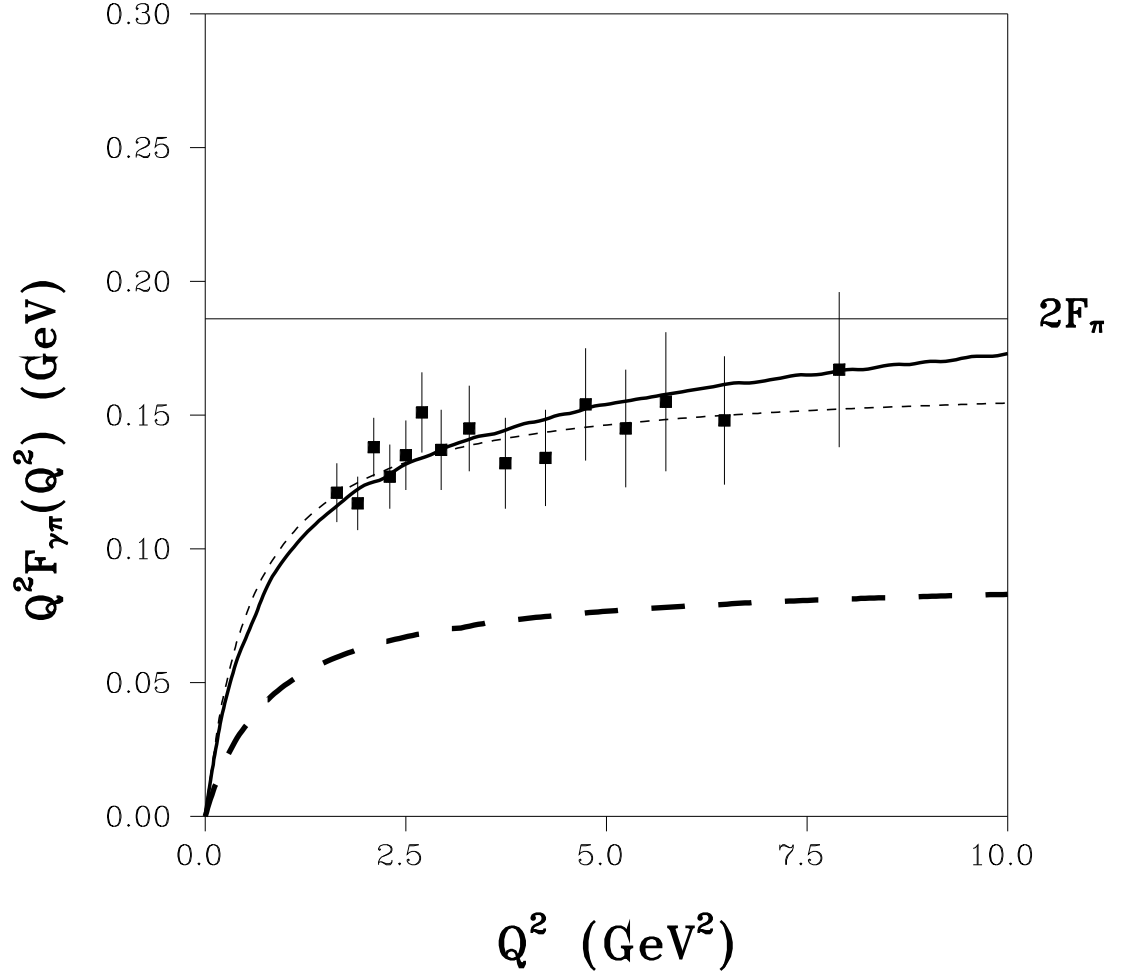


FIG. 4. Transition pion form factor. Solid curve represents a result of the model of induced nonlocal quark currents. Long dashed line - calculation without taking into account the spin-field interaction. Experimental fit [29] is given by short dashed line, and Brodsky-Lepage limit [1] ($\approx .186$ Gev) is shown by solid straight line;

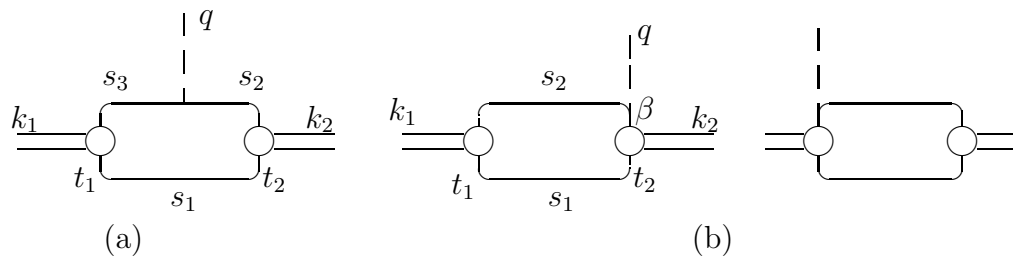


FIG. 5. The triangle (a) and bubble (b) diagrams for pion charge form factor.

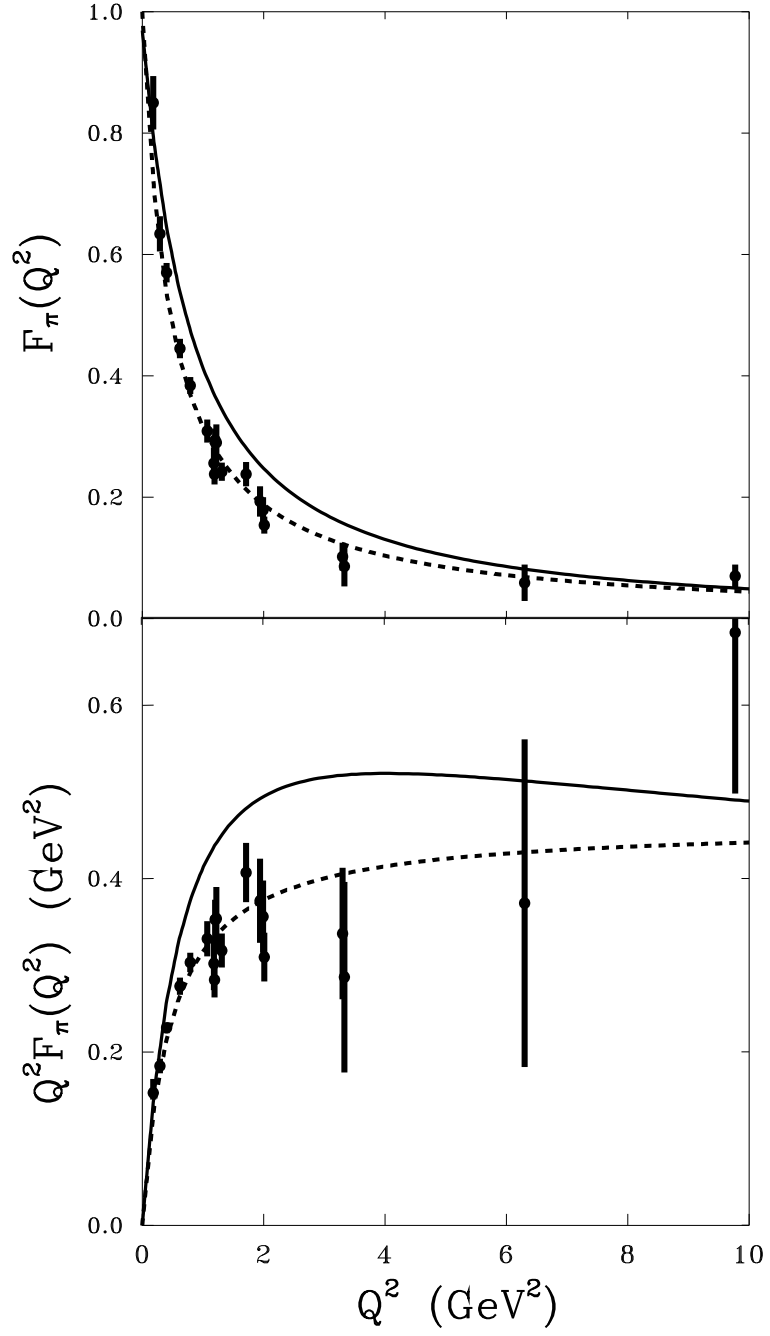


FIG. 6. The pion charge form factor $F_\pi(Q^2)$ calculated in the present model (solid line) compared with experimental fit (dashed line)

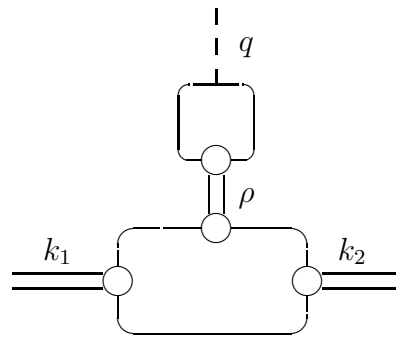


FIG. 7. The diagram with ρ -meson exchange.